



**University of Venda**

SCHOOL OF ENVIRONMENTAL SCIENCES

DEPARTMENT OF ECOLOGY AND RESOURCE MANAGEMENT

**Removal of Congo red dye from aqueous solution using a clay based  
nanocomposite**

BY

**Rasilingwani Tshimangadzo Edward,**

Student number: 11613622

**Supervisor: Prof JR Gumbo**

**Co-supervisor: Dr. V Masindi (Pr. Nat. Sci.) (Council for Scientific and Industrial  
Research (CSIR))**

**A Dissertation submitted to the Department of Ecology and Resources Management,  
University of Venda, in fulfilment of the requirement of Masters of Earth Sciences in  
Environmental Science**

**May 2018**

## DECLARATION

I, **Rasilingwani Tshimangadzo Edward**, hereby declare that this thesis submitted for the Master of Environmental Sciences in Department of Ecology and Resources Management at the University of Venda by me is my own work, that it has not been submitted for any degree or examination at this or any other Institution, and that all the sources I have used or quoted have been indicated and duly knowledged by complete references.

Signature..... Date.....

## DEDICATIONS

This Thesis is dedicated to my entire family:

- **Rasilingwani Rotondwa**
- **Rasilingwani Rabelani**
- **Rasilingwani Thabelo**
- **Rasilingwani Tshililo Edson**
- **Mathegu Muvhulawa**
- **Mathegu Nyambeni**
- **Gundula Mpho**

These people are crucial in my life, and they are the reason why I work hard.

## ACKNOWLEDGEMENTS

Firstly I would like to thank the **Almighty God** for the strength and wisdom he gave me to overcome this Thesis.

I would like to express profound gratitude and sincere thanks to my supervisors **Prof. JR Gumbo and Dr. V Masindi** for their guidance, facilitation, supervision and most assistance through-out this project.

I would also like to give special thanks to **Dr. V Masindi** for giving me magnificent, courageous and hardworking Lab assistances, **Miss Muedi KL and Ngulube T.** Your support, guidance and advices during those sleepless nights are remarkable.

I wish to extend my sincere thanks to **Prof. W.M Gitari** and support staff of Department of Ecology and Resources Management for their continuous support in terms of Lab materials and space.

Lastly, I would also like to thank the financial support that I got from **Water Research Commission (WRC)** for funding this research; it was not going to be easy without your financial support.

## TABLE OF CONTENTS

<b>DECLARATION</b> .....	<b>i</b>
<b>DEDICATIONS</b> .....	<b>ii</b>
<b>ACKNOWLEDGEMENTS</b> .....	<b>iii</b>
<b>TABLE OF CONTENTS</b> .....	<b>iv</b>
<b>LIST OF TABLES</b> .....	<b>vii</b>
<b>LIST OF FIGURES</b> .....	<b>viii</b>
<b>ABSTRACT</b> .....	<b>x</b>
<b>CHAPTER ONE</b> .....	<b>1</b>
<b>INTRODUCTION</b> .....	<b>1</b>
1.1 Background information .....	1
1.2 Problem statement .....	3
1.3 Objectives.....	4
1.3.1 Main Objective.....	4
1.3.2 Specific Objectives .....	4
1.4 Hypothesis.....	4
1.5 Structure of the thesis.....	4
<b>CHAPTER: TWO</b> .....	<b>5</b>
<b>LITERATURE REVIEW</b> .....	<b>5</b>
2.0 Introduction .....	5
2.1 Dyes.....	5
2.2 Sources of dyes.....	6
2.3 Uses of dyes .....	6
2.4 Impacts of dyes.....	8
2.4.1 Environmental effects .....	8
2.4.2 Health effects .....	8
2.5 Remediation technologies of dyes .....	9
2.5.1 Adsorption.....	9
2.5.2 Filtration.....	10
2.5.3 Ion-exchange.....	11
2.5.4 Solidification.....	11

2.5.5	Bio-sorption/biodegradation .....	11
2.6	Adsorption of Congo red dye .....	12
2.7	The relationship between surface area and adsorption capacity .....	12
2.8	Legal requirement and water quality .....	13
2.9	Mathematical modelling.....	13
2.9.1	Modelling of CR removal and adsorption capacity .....	13
2.9.2	Adsorption Kinetics .....	14
2.9.3	Adsorption isotherms .....	15
2.9.4	Thermodynamic studies .....	16
2.10	Concluding remarks .....	17
<b>CHAPTER THREE .....</b>		<b>18</b>
<b>MATERIALS AND METHODS .....</b>		<b>18</b>
3.1	Sampling.....	18
3.2	Preparation of the feed materials.....	18
3.3	Synthesis of the clay-based-nanocomposite.....	18
3.4	Characterization of feed and recovered materials .....	19
3.4.1	Mineralogical composition .....	19
3.4.2	Morphological analysis.....	19
3.5	Batch experimental studies.....	19
3.5.1	Effect of contact time .....	19
3.5.2	Effect of dosage .....	20
3.5.3	Effect of species concentration .....	20
3.5.4	Effect of solution pH .....	21
3.5.5	Effect of temperature .....	21
3.6	Removal of CR at optimized conditions .....	21
3.7	Desorption and regeneration studies .....	21
3.8	Computation of CR % removal and adsorption capacity .....	21
3.9	Adsorption Kinetics.....	22
3.9.1	Pseudo-first-order kinetic .....	22
3.9.2	Pseudo-second-order kinetic.....	22
3.10	Adsorption isotherms .....	22
3.10.1	Langmuir adsorption isotherm.....	22
3.10.2	Freundlich adsorption isotherm .....	23
3.11	Adsorption thermodynamics .....	24
3.12	Desorption study .....	24

3.13	Determination of Point of Zero Charge (PZC).....	25
<b>CHAPTER FOUR.....</b>		<b>26</b>
<b>RESULTS AND DISCUSSIONS .....</b>		<b>26</b>
4.1	Characterisation.....	26
4.1.1	Mineralogical analysis .....	26
4.1.2	Morphological analysis.....	27
4.2	Batch adsorption experiments .....	28
4.2.1	Effect of contact time .....	28
4.2.2	Effect of adsorbent dosage .....	29
4.2.3	Effect of CR concentration .....	30
4.2.4	Effect of solution pH and the point of zero charge.....	31
4.2.5	Effect of temperature .....	32
4.3	Adsorption kinetics .....	33
4.3.1	Pseudo-first-order kinetic .....	33
4.3.2	Pseudo-second-order kinetic.....	34
4.3.3	Intra-particle diffusion model.....	35
4.4	Adsorption isotherms .....	36
4.4.1	Langmuir and Freundlich adsorption isotherm .....	36
4.4.2	Thermodynamics .....	39
4.5	Treatment of authentic dye effluence.....	42
4.6	Desorption and regeneration studies .....	43
4.7	Comparison of the synthesized nanocomposite with other adsorbents.....	44
4.8	Mechanisms of Congo Red (CR) removal .....	45
<b>CHAPTER FIVE .....</b>		<b>47</b>
<b>CONCLUSIONS AND RECOMMENDATIONS.....</b>		<b>47</b>
5.1	Conclusions .....	47
5.2	Recommendations .....	48
<b>REFERENCES.....</b>		<b>49</b>

## LIST OF TABLES

<b>Table 2.1:</b> Classification of dyes based on their application.....	7
<b>Table 4.1:</b> Pseudo-first-order and second-order kinetic models parameters for the adsorption of CR onto bentonite clay, pre-treated magnesite, and their nanocomposite.....	35
<b>Table 4.2:</b> Intra-particle diffusion model parameters for the adsorption of CR onto bentonite clay, pre-treated magnesite, and their nanocomposite .....	35
<b>Table 4.3:</b> Langmuir and Freundlich adsorption isotherm parameters for the adsorption of CR onto bentonite clay, pre-treated magnesite, and their nanocomposite .....	39
<b>Table 4.4:</b> Thermodynamics for the adsorption of CR onto bentonite clay, pre-treated magnesite, and their nanocomposite .....	41
<b>Table 4.5:</b> Comparison of the efficiency of bentonite clay, pre-treated magnesite, and their nanocomposite with other adsorbents used for CR removal.....	45

## LIST OF FIGURES

<b>Figure 2.1:</b> Congo red chemical structure .....	12
<b>Figure 3.1:</b> Standard CR dye solution concentration using UV-VIS spectroscopy .....	20
<b>Figure 4.1:</b> Mineralogical characteristics of bentonite clay, pre-treated magnesite, and their nanocomposite.....	26
<b>Figure 4.2:</b> Morphological characteristics of bentonite clay, pre-treated magnesite, and their nanocomposite .....	27
<b>Figure 4.3:</b> Variations in percentage removal of CR as a function of contact time.....	28
<b>Figure 4.4:</b> Variations in percentage removal of CR as a function of dosage .....	29
<b>Figure 4.5:</b> Variations in percentage removal of CR as a function of adsorbate concentration .....	30
<b>Figure 4.6:</b> Variations in percentage removal of CR as a function of pH and the PZC of different feed materials are also shown. ....	31
<b>Figure 4.7:</b> Variations in percentage removal of CR as a function of temperature.....	32
<b>Figure 4.8:</b> Pseudo-first-order kinetic for the adsorption of CR dye using bentonite clay, pre-treated magnesite, and their nanocomposite .....	33
<b>Figure 4.9:</b> Pseudo-second-order kinetics for the adsorption of CR dye using bentonite clay, pre-treated magnesite, and their nanocomposite. ....	34
<b>Figure 4.10:</b> Intra-particle diffusion model for the adsorption of CR from aqueous solution using bentonite clay, pre-treated magnesite, and their nanocomposite. ....	36
<b>Figure 4.11:</b> Langmuir adsorption isotherms for the adsorption of CR from aqueous solution using bentonite clay, pre-treated magnesite, and their nanocomposite. ....	37
<b>Figure 4.12:</b> Freundlich adsorption for the adsorption of CR by bentonite clay, pre-treated magnesite, and their nanocomposite .....	38
<b>Figure 4.13:</b> Thermodynamics for the adsorption of CR ions by bentonite clay, pre-treated magnesite, and their nanocomposite. ....	40

**Figure 4.14:** Efficiency of the synthesized nanocomposite for the removal of CR from synthetic and printing industry .....42

**Figure 4.15:** Desorption of CR from bentonite clay, pre-treated magnesite, and their nanocomposite using five different desorption agents. ....43

**Figure 4.16:** Desorption cycles of CR from bentonite clay, pre-treated magnesite, and their nanocomposite matrices using methanol. ....44

## ABSTRACT

In this study, the efficacy of bentonite clay, pre-treated magnesite and their nanocomposite on the removal of Congo red dye from aqueous solution was explored. Batch experimental approach was a technique used to fulfil the goals of this study. A number of operational parameters were optimised, and they include effects of shaking time, adsorbent dosage, initial CR dye concentration, initial solution pH and temperature. Findings of the study revealed that the optimum conditions that are suitable for the removal of CR dye are 20 minutes, 0.5 g of dosage, 120 mg/L, 250 rpm, and pH = 7. This has achieved > 99% removal efficacy of CR dye for the nanocomposite and reduced it to below the South African National Standard (SANS) 241 water quality specifications. Furthermore, kinetic studies revealed that bentonite clay, pre-treated magnesite, and their nanocomposite fitted very well to pseudo-second-order kinetics than pseudo-first-order kinetics. The regression analysis was observed to be 1, 0.9, and 0.9 for bentonite clay, pre-treated magnesite, and their nanocomposite respectively. Adsorption isotherms indicated that CR removal by bentonite clay, pre-treated magnesite, and their nanocomposite fitted well to Langmuir adsorption isotherm than the Freundlich adsorption isotherm hence indicating mono-layer adsorption. Thermodynamic values for CR removal were observed to be:  $\Delta H^0$  (kJ mol<sup>-1</sup>) = 43.86, 30.67, and 24.88 for bentonite clay, pre-treated magnesite, and their nanocomposite respectively. This indicates that the reaction is endothermic. The positive  $\Delta S^0$  (kJ mol<sup>-1</sup> K<sup>-1</sup>) values for bentonite clay and 25 °C for pre-treated magnesite confirms that there is an increase in the degree of randomness at solid/solution interface during the removal of CR ions from aqueous solution. The negative values of  $\Delta G^0$  (kJ mol<sup>-1</sup>) for 40 – 70 °C on bentonite and the entire range for the nanocomposite suggest the spontaneity and feasibility of CR adsorption whereas the positive  $\Delta G^0$  (kJ mol<sup>-1</sup>) for bentonite clay suggest a non-spontaneous nature of adsorption. As such, pre-treated magnesite/bentonite clay nanocomposite demonstrated superior adsorption capacity in relation to individual materials and other materials reported in literature.

**Keywords:** Congo red Dye; Bentonite clay; Calcined cryptocrystalline magnesite; Decolouration; Adsorption; Modelling

## CHAPTER ONE

### INTRODUCTION

#### 1.1 Background information

Dyes impart colour to a variety of man-made and natural resources. They are also regarded as one of the outstanding components in pigments and chromatic science. They form part of the aesthetic value of the environment (Ngulube et al., 2017, Mahmoud et al., 2018). More prevalently, dyes are widely used in industries such as textile, cosmetics, pulp and paper, paints, pharmaceuticals, and carpet, as well as in printing sectors (Hu et al., 2018, Zhang et al., 2018, Ziane et al., 2018). Even though they possess some outstanding benefits, many dyes are toxic and biologically non-degradable due to complex chemical structures and the presence of aromatic rings in their structure and matrices (Ausavasukhi et al., 2016, Sasmal et al., 2017, Miandad et al., 2018). Most of the azo dyes used contain an azo-bond ( $-N=N-$ ) connected with the aromatic ring which imparts their stability, hence resisting any form of degradation (Alver et al., 2017, Chahkandi, 2017, Chawla et al., 2017). For example, Azo dyes contain one or more azo groups with an aromatic ring and sulfonate group, and they can be transformed into more hazardous substances under anaerobic conditions (Sasmal et al., 2017, Zheng et al., 2018).

Within the various azo dyes, Congo red dye (CR) is very much important for its wide use in textile, wool, silk, printing, and food industries due to its high solubility and stability. CR is also used for diagnosis of amyloidosis, as a biological stain in medicine and also as an indicator in acidic medium (Sasmal et al., 2017, Ziane et al., 2018). Despite its outstanding benefits, CR is also regarded as one of the prime pollutants in the biosphere due to the nature of toxicity and the magnitude of its impact to living organisms. The discharge of CR dye contaminants into natural or engineered water bodies has caused serious environmental problems in recent years, since CR is highly toxic to aquatic life and hard to be degraded in natural environments (Mahmoud et al., 2018). Therefore, it is essential to remove these dyes from wastewater prior release to different environmental compartments (Ngulube et al., 2017, Xu et al., 2018). CR has been documented to be very toxic for living organisms on exposure because it can cause allergies, dermatitis, skin irritation, and mutation in human bodies (Toor and Jin, 2012, Toor et al., 2015). Toxicological studies also highlighted that CR may cause eye and skin irritation, gastrointestinal irritation, vomiting and diarrhoea (Sasmal et al.,

2017). Prolonged exposure to CR may also lead to several forms of cancer because it easily gets metabolized to benzidine that has carcinogenic effects and causes liver tumour for women (Miandad et al., 2018). Unlike natural dyes, commercial dyes, such as CR, have complex structures and are not easily degraded, hence making them persistent in different environmental compartments (Hu et al., 2018, Zhang et al., 2018). The presence of azo dyes in water blocks sun light and prevents gas solubility, hence affecting the photosynthesis of aquatic plants and also causes suffocation of flora and fauna (Ausavasukhi et al., 2016, Ngulube et al., 2017).

Due to a rapid growth in population size and a rising demand for clean water resources, environmental regulations are becoming more stringent with regard to environmental protection hence requiring industries to treat their effluents prior to releasing them to different spheres of the environment (Ngulube et al., 2017). Moreover, wastewater-containing dyes are also difficult to treat using conventional wastewater treatment methods because dyes are very stable organic compounds recalcitrant to chemical or biological degradation and they are resistant to oxidizing agents, aerobic digestion, heat and light (Sasmal et al., 2017, Ziane et al., 2018). As a result, research studies are in a quest for pragmatic solutions for the decolouration of such effluents. To minimize their environmental impacts and pollution, a wide range of methods has been developed, piloted and implemented for decolouration of effluents (Ngulube et al., 2017). These technologies are mainly based on physicochemical methods such as adsorption using different adsorbents (Ngulube et al., 2017), coagulation and precipitation (Gao et al., 2007, Zhao et al., 2014, Dhal et al., 2015), membrane filtration (Ghaemi et al., 2015, Zhao and Wang, 2017), photo-catalysis (Yola et al., 2014, Hou et al., 2017), oxidation processes (Panizza and Cerisola, 2008, Kumar et al., 2011), electrochemical oxidation (Panizza and Cerisola, 2008), decomposition by microbiological or enzymatic components (Karthikeyan et al., 2015, Mahmoud et al., 2018) and ion exchange (Chen et al., 2011, Mohy Eldin et al., 2016, Suteu et al., 2016). Amongst all the techniques used for the removal of colour in water, adsorption has received paramount attention in depollution science. This is attributed to its high efficiency, easiness to operate, regenerate-ability and design-ability. Various and common adsorbents are widely used and they include: activated carbon (Yang et al., 2008, Belhachemi et al., 2009), clays (De León et al., 2013, Ngulube et al., 2017), and metal oxides and hydroxides (Hu et al., 2012, Kanade et al., 2017), and these have been studied for the adsorptive removal of dyes from contaminated water. However, many of these adsorbents fail to fully meet the requirements as stipulated by different end-

users, such as good adsorption selectivity or high adsorption capacity. As such, the quest for effective, locally available, and efficient adsorbent is still an issue of prime concern to colloidal and adsorption scientists.

This study was therefore developed with the aim of removing Congo Red (CR) from an aqueous system using calcined and ball milled cryptocrystalline magnesite/Ca-bentonite clay composite as an adsorbent. Mg and clay-based materials have been widely applied for decolouration of water. Xu et al. (2018) evaluated the adsorptive removal of an anionic dye Congo red by flower-like hierarchical magnesium oxide (MgO)-graphene oxide composite microspheres, and showed high adsorption capacity of 227.7 mg/g. Toor et al. (2015) investigated the use of activated natural bentonite as a cost-effective adsorbent for removal of Congo-red in wastewater. Their study reported that the maximum Congo red adsorption of approximately 7.0 mg/g was obtained in their study. Ziane et al. (2018) evaluated the ability of single and binary adsorption of reactive black 5 and Congo red on modified dolomite. Their study revealed that modified dolomite has the adsorption capacity of 72.4 mg/g. This is an indication that magnesium and calcium based materials have been used for the removal of colour. In light of the above, the use of MgO-rich magnesite and bentonite clay for the removal of CR has not been explored. As such, this is the first study in design and execution.

## 1.2 Problem statement

Industrial effluents have created a serious problem to the environment, particularly disposal of colored or dyed wastewater (Nandi et al., 2008). Dyed contaminated wastewater contains colored compound from residues of dyes such as benzidine, naphthalene and other aromatic compounds (Oladipo and Gazi, 2014). Reactive dyes are extensively used due to their high reactivity and good color resilience (Venkataraman, 1972). However, they are harmful to aquatic environment especially for aquatic organisms if they are discharged through inadequate treatment (Dogan et al., 2007). Some dyes contain heavy metals like: copper, nickel, mercury, chromium and cobalt as the functional group of dyes (Widujanti, 2009). Furthermore, because of the inhibition of sunlight penetration into the water as dye color absorb and reflect sunlight, bacterial and benthic organism growth in water and photosynthesis of aquatic plants may be disrupted by discharged dyes (Roshan, 2015). Beyond these, some dyes such as Congo red have been classified as a hazardous substance with the ability of causing irritation of the gastrointestinal tract, shortness of breath and

coughing(Rui et al., 2013). As such, this dyes need to be removed prior contamination of aquatic ecosystems.

### 1.3 Objectives

#### 1.3.1 Main Objective

The main objective of this study was to evaluate the removal of Congo red dye from aqueous solution using bentonite clay, pre-treated magnesite and their nanocomposite.

#### 1.3.2 Specific Objectives

To achieve the main objective of this study, the following specific objectives were developed and they are:

- To examine the physicochemical characterization of materials used in this study.
- To optimize the removal of Congo red from aqueous solution using bentonite clay, pre-treated magnesite and their nanocomposite.
- To point out mechanisms that are governing the removal of Congo red from aqueous solution using bentonite clay, pre-treated magnesite and their nanocomposite.
- To compare the quality of product water with South African National Standard (SANS) 241 specifications.

### 1.4 Hypothesis

Bentonite clay/pre-treated magnesite nanocomposite has superior efficacy for Congo Red removal in relation to bentonite clay and magnesite individually.

### 1.5 Structure of the thesis

This thesis is characterized of six chapters: **Chapter 1:** Introduction to the purpose of the study. **Chapter 2:** Concise literature review about dyes and their remediation technologies. **Chapter 3:** Materials and methods used to achieve the goals of this study. **Chapter 4:** Facile synthesis of bentonite clay/pre-treated magnesite nanocomposite and its use for the removal of Congo red from aqueous solution: kinetics, isotherms, thermodynamics, and mechanisms. **Chapter 5:** conclusions and recommendations. **References** will also be included to acknowledge the used literature.

## CHAPTER: TWO

### LITERATURE REVIEW

An in-depth explanation of the dyes problem and solutions is given: their sources, uses, impacts, and their remediation technologies. Legal requirements and water quality were discussed. Furthermore, for removal percentage and adsorption capacity, mathematical modelling were evaluated. In order to extremely understand the nature of adsorption, thermodynamics studies were evaluated. The analysis of statistical errors, coefficient of determination ( $R^2$ ), residual sum of square error (RSS) and standard error (SE) are evaluated for adsorption systems.

#### 2.0 Introduction

This chapter presents the overview of dyes, mainly concentrating on the anionic and cationic dyes, their impacts to fauna and flora, and treatment technologies. It will also focus on dyes and their sources, their beneficial uses, health and environmental impacts of dyes, remediation technologies and water quality requirements.

#### 2.1 Dyes

Ever since pre-historic time, man has been fascinated to color the objects of daily use employing inorganic salts or natural pigments of vegetables, animal, and mineral origins. These coloring substances, known as dyes, are chemical compounds used for coloring fabrics, leather, plastic, paper etc. and also produce inks and artistic colors (Singh and Bharati, 2014).

Dyes are colored compounds appropriate for adding a color or change the color of something (Nandi et al., 2008). They are widely used in the textile, pharmaceutical, food, cosmetics, plastics, paint, ink, photographic and paper industries (Radha et al., 2005). Dyes are colored substances which are soluble or go into solution during the application process and impart color by selective absorption of light, as they are generally known to be stable to light, heat and oxidizing agents and are usually non-biodegradable (Broadbent, 2001; Nandi et al., 2008). In the application medium, usually in water, at some points during the coloring process, dyes usually exhibit some substantively for the material being dyed and are absorbed from aqueous solution (Broadbent, 2001). Dyes can generally be described as colored

substances that have affinity to the substrates to which they are being applied(Pereira and Alves, 2012). Dyes are soluble and can go through a process which, at least temporarily, destroys any crystal structure by absorption, solution and mechanical retention, or by ionic or covalent chemical bonds(Nwokonkwo, 2013).

## **2.2 Sources of dyes**

Dyes are categorized in two types, i.e., natural and synthetic. Synthetic dyes are based on petroleum compound, whereas natural dyes are obtained from plant, animal and mineral matters(Singh and Bharati, 2014). Natural dyes are obtained from natural sources, mostly are of plant origin and extracted from roots, wood, bark, berries, lichens, leaves, flowers, tuna, and seeds. Others come from insects, shellfish, and mineral compounds. Natural dyes were the only source of color for textile, leather, basketry, and other materials until synthetic dyes were developed in the latter half of the nineteenth century, as thousands of natural color substances were very less significant commercially(Casselmann, 1980). Natural dyes includes: jackfruit, onion, eucalyptus, turmeric, weld and henna(Dawwod and Sen, 2014). Due to their failure to meet the industrial demand and population increase with the advancement and development in time and technology, people are moving away from natural dyes to synthetic dyes. However, natural dyes remain important for artists, craftspeople, and niche producers(Liles, 1990). Synthetic dyes are synthesized dyes primarily made from aniline or chrome dyes obtained from chemical processes. They include: basic, acid, direct, vat, reactive and disperse dyes(Chen et al., 2016). Synthetic dyes exhibit advantages such as high tinctorial strength, wide range shade, relatively economical and moderate substantively. Almost all the colors that we see today are synthetic dyes, as they are widely used for dyeing and printing in a broad range of industries. Synthetic dyes can be named according to the chemical structure of their particular chromosphoric group, which include; diphenylmethane derivatives, triphenylmethane compounds, oxazine compounds and azo dyes. Within the above mentioned chromosphoric group, azo dyes are one of the most popular varieties of synthetic dyes, due to their versatility and simplicity to synthesize, and are the largest group of colorants, constituting 60-70 % of all organic dyes produced in the world(Roshan, 2015).

## **2.3 Uses of dyes**

Dyes have a variety of application and are used as a coloring agent for a wide range of substances. Dyes are widely used to give color to fabrics and plastics(Zollinger, 1991). They are also used in food industry, printing and leather industry(Srinivasan and Sorial, 2009).

Recently, dyes have gained popularity in hair coloring (Khenifi et al., 2007). Overall, dyes have been broadly applied in virtually all industries, such as textile, cosmetics, pulp and paper, paint, pharmaceutical, carpet and printing, leather and food. Classification of dyes based on their application is shown in **Table 2.1**.

**Table 2.1:** Classification of dyes based on their application (Zollinger et al., 1991; Banat et al., 1996; Forgacs et al., 2004; Martinez-Hutile and Brillas, 2009)

Type of dye	Example	Application
Acid dyes	Methyl orange, Methyl Red Orange I, Orange II and Congo red	Wool, Silk, polyurethane fibers, nylon and printing (Martinez - Hutile and Brillas, 2009)
Basic dyes	Aniline yellow, Butter yellow methylene and malachite green	Reinforced nylon, polyesters (Forgacs et al., 2004)
Direct dyes	Martius yellow and Congo red	Cotton, Rayon, Wool, Silk and Nylon (Banat et al., 1996)
Disperse dyes	Celliton fast pink B, Celliton fast blue B	Synthetic polyamide, fibers, polyesters, nylon and polyacrylonitries (Forgacs et al., 2004)
Ingrain azo dyes	Para red	Cotton (cellulose), silk, Nylon, Polyester, coloring agent in food (Banat et al., 1996)
Vat dyes	Indigo, Tyrian purple, Benzanthrone	Wool, coloring agent in food (Zollinger, 1991)
Mordant	Alizarin	Cotton and wools (Martinez-Hutile and Brillas, 2009)

## **2.4 Impacts of dyes**

### **2.4.1 Environmental effects**

Despite their beneficial uses, the discharge of dyes from industries, especially textiles, paper, paints and cosmetics, into the water environment is undesirable due to their color. Also, as dyes enter the aquatic environment, they break down into compounds which are toxic, carcinogenic or mutagenic to life due to them being composed of carcinogens such as benzidine, naphthalene and other aromatic compounds (Mittal et al., 2005a).

The great concern with dyes is their absorption and reflection of sunlight entering into water (Zehra et al., 2009). Sunlight absorption diminishes photosynthetic activity of algae and it seriously disrupts the aquatic food chain due to the presence of dyes in the water, meanwhile, affecting the quality of water, hence damaging the scenic beauty of the lake, river or stream (Roshan, 2015). Azo dyes in the aquatic environment pose severe toxic impacts on the microorganisms, which could be carcinogenic and mutagenic (Chen et al., 2016). They enter the body by ingestion and are metabolized by intestinal microorganisms causing DNA damage (Crini and Badot, 2008). The presence of heavy metals in dyes used in printing industries and pigments such as titanium oxide, chromate, molybdenum and iron used as pigments, aluminium and brass used in metallic inks have posed serious environmental problems such as soil pH fluctuations (Mittal et al., 2005b; El-Latif et al., 2010).

### **2.4.2 Health effects**

Dyes are toxic due to the presence of benzene and aromatic ring in their structure (Khenifi et al., 1996). In humans, the contact with colored wastewater may cause serious health problems and hazards-induced disease, such as allergies, skin diseases, mutation and cancer (Bhatnagar and Jain, 2005; Chatterjee et al., 2009). Heavy metal compounds such as molybdenum, chromate, and titanium oxide have the ability to leach into underground waters, which could lead to serious health issues in both human and wildlife (Masindi et al., 2015a). Dyes can also lead to the dysfunction of kidneys, liver, brain and central nervous system (Ozcan and Ozcan, 2004). It has been reported that due to the toxicity of this azo dye and its inappropriate discharge, skin diseases and respiratory problems have been found amongst many dyes factory workers in India. Other problems include; cardioid effects due to inhalation of finely ground metals which result from ink manufacturing (Roshan, 2015). Furthermore, azo dyes are unsafe dyes which not only possess extremely toxic properties affecting the cells of

mammals, but also possess the power to cause anaphylactic shocks in humans and are potentially carcinogenic (Chen et al., 2016).

## **2.5 Remediation technologies of dyes**

Environmental impacts mitigation and dyes control are the main focus for the best practice of sustainable environment within aquatic ecosystems. However, due to high cost, sludge disposal and efficiency at high concentration of various convectional treatment methods such as ozonation (Koch et al., 2002), chemical precipitation (Liu et al., 2002), reverse osmosis (Gupta et al., 2007), coagulation/flocculation (Pollock, 1973), membrane separation and solvent extraction for removal of dyes effluents, it has been noted that adsorption is the most successful and most commonly used method for the removal of industrial dye effluents (Sachdava & Kumar, 2009).

### **2.5.1 Adsorption**

Adsorption processes have been noted to be the most applied treatment method in industries, and consequently the most studied (Charlie et al., 2000). Adsorption is commonly defined as the mass transfer of a substance (adsorbate) from liquid or gaseous phase onto the solid interface (adsorbent) and becomes attached by physical or chemical interactions (Kurniawan et al., 2006). Thus, adsorption can either be physical or chemical in nature, and frequently involves the two (Cheremisinoff and Morresi, 1978). Several adsorbents have been used to treat industrial dyed wastewaters, and they include:

#### **2.5.1.1 Activated carbon**

It is a well-known adsorbent and has been proven to be useful for removal of heavy metals. Nevertheless, the application of activated carbon for wastewater treatment is not feasible due to its high price and cost associated with the regeneration as a result of high-degree of losses in real process (Febrianto et al., 2009).

#### **2.5.1.2 Zeolites**

These are aluminosilicates minerals containing exchangeable alkaline and alkaline metal cations (usually Na, K, Ca and Mg), as well as water in their structural framework. Zeolites have high ion-exchange and size selective adsorption capabilities, as well as thermal and mechanical abilities (Weng et al., 2009). However, zeolites become unstable at high pH (Benkli, et al., 2005) and for this reason, chemicals are added to adjust the pH, which in turn makes this process expensive and the process of regenerating zeolites packed bed dumps salt

water into the environment. Furthermore, the use of zeolites does not reduce the level of most organic compounds (Johnson, 2005).

### **2.5.1.3 Activated alumina**

It is referred to as a filter media made by treating aluminum ore so that it becomes porous and highly adsorptive. Activated alumina removes a variety of contaminants that often co-exist with fluoride, such as excessive arsenic and selenium (Faroogi et al., 2007). The main disadvantage of activated alumina is that the adsorption efficiency is highest only at low pH and contaminants like arsenites must be pre-oxidized to arsenates before adsorption.

However, due to difficulties and costs involved in regeneration by the above mentioned adsorbents, clays are considered as the best alternative which is of low cost. Recent investigations have also gained focus on the use of clays for dyes removal from industrial wastewaters since clay derivatives can be easily prepared and regenerated (Gu et al., 2010). Therefore, calcined and ball milled cryptocrystalline magnesite/Ca bentonite clay nanocomposite was tested in this present study for removal of congo red dye from aqueous solutions.

### **2.5.1.4 Calcined magnesite and bentonite clay composite**

Cryptocrystalline magnesite has been an endemic mineral in South Africa. It has been widely used for wastewater treatment. Bentonite clay has also been reported to be the only low cost material that is widely used in numerous fields of material science technology and the utilization of this clay material for treatment of wastewater containing hazardous substances has received great attention (Bhatnagar et al., 2011). A number of studies have used it for acid mine drainage treatment (Masindi et al., 2015a), removal of fluoride (Masindi et al., 2015b), boron (Masindi and Gitari, 2016) and as a precursor for struvite synthesis. However, there are limited studies on removal of Congo Red (CR) dye in wastewater streams. This is one study in design and execution to evaluate the feasibility of removing CR from printing industry wastewater effluents.

## **2.5.2 Filtration**

Filtration is usually employed to remove any particulate matter present in the wastewater. Membrane filtration has high affinity towards the treatment of dye effluent. Most importantly, membrane filtration can be used for continuous removal of dyes from dyes effluent (Xu and Lebrum, 1999). Unlike other physico-chemical methods, filtration is

resistant to temperature, chemical and microbial attack. The treated dye effluent can be recycled within the textile industry; however, reuse of water treated by filtration is not very feasible (Mishra and Tripathy, 1993). On the flip side, the disposal of sludge formed during treatment is a major problem (Letterman et al., 1999). In addition, filtration involves high capital cost and tendency of membranes to clog, which then affects the performance of the filtration process (Robinson et al., 2001).

### **2.5.3 Ion-exchange**

Exchange of cations or anions between pollutants and the media is referred to as ion-exchange. Ion-exchangeable materials are generally resins (natural polymers with a variety of anionic functional groups for attachment of exchangeable ions) (FRTR, 2012). Ion exchange finds extensive application for the softening of hard water. However, the use in dye effluent is limited (Slokar and Le Marechal, 1997). The advantages of ion exchange include the availability of a wide range of resins for specific application and no loss of sorbent. Ion exchange can be used for the removal of soluble dyes; however, it is ineffective for insoluble dyes (Mishra and Tripathy, 1993). Drawbacks of ion exchange are high capital cost and expensive organic solvents (Robinson et al., 2001).

### **2.5.4 Solidification**

Solidification is one of the best known waste fixation processes that offer reduction in mobility of pollutants in the environment both chemically and physically. In this method, contaminants are enclosed or physically bound within a stabilized mass. Though mass reduction in contaminants does not occur in this technique, reduced mass flux and mobility to receptors effectively removes the pollutants pathway. Mostly, this technology has limited effectiveness against pesticides and organics, except for vitrification and asphalt batching. Compared to biopiles or monitored natural attenuation, it has a short treatment time scale with an ability to remediate a wide range of mixed contaminants. Generally, environmental conditions affect the long-term pollutant immobilization. This treatment, however, is site-specific where residual long-term liability is observed. Inhibitory substances like free-phase solvents and oils limit the success of this system (RAAG, 2000; FRTR, 2012).

### **2.5.5 Bio-sorption/biodegradation**

Biological treatment of wastewater for the removal of pollutants is widely used. The application of microorganisms for the degradation of dyes started almost two decades ago. The removal of synthetic dyes by microorganisms is a simple method but involves a complex

mechanism (Forgacs et al., 2004). The growth of microorganisms is complex and requires in-depth knowledge of the suitable environment in which microorganisms can grow. Biodegradation possesses lots of advantages, including 1) the low-cost process: low infrastructure and operating costs, 2) complete mineralization with non-toxic end products, and 3) no other chemicals which are associated with potential health hazards (Stoltz, 2001).

## 2.6 Adsorption of Congo red dye

Congo red dye is an azo dye and a sodium salt of benzidinediazo-bis-1-naphthylamine-4-sulphuric acid with a molecular formula of  $C_{32}H_{22}N_6Na_2O_6S_2$ , a molecular weight of 696.663219 and  $\lambda_{max} = 614$  nm (Roshan, 2015). It is an acidic anionic dye and considered as one of the highly soluble secondary diazo dye. **Figure 2.1** below shows the chemical structure of Congo red dye:

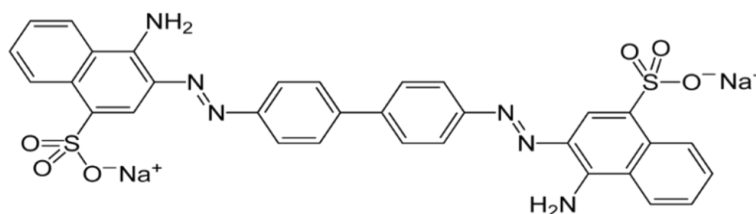


**Figure 2.1:** Congo red chemical structure (Roshan, 2015).

Magnesite-bentonite clay composites, as adsorbents for congo red dye in solution, resulted into precipitation of dye by magnesite as it is composed of two cations which adsorb single cation of sodium and also adsorbed in bentonite clay via ion exchange, and the dye settled in between its layers as bentonite are known to have high surface area (Masindi et al., 2014a; Masindi et al., 2015b).

## 2.7 The relationship between surface area and adsorption capacity

The major reason for the high adsorption capacity of clay materials is their high surface areas. Cadena et al (1990) reported that a material with a higher surface area will have a higher adsorption capacity as compared to a material with low surface area. Although this may not always be the case, a number of studies have documented that the surface area of a material is directly proportional to the adsorption capacity of the material, with clays being the most documented materials to have great surface areas (Sarma, et al. 2016; Santos and Boaventura, 2016; Ngulube et al., 2016). Adsorbents with great pore size, high pore volume and high mechano-chemical strength have been noted to lead to high adsorption of dyes and other pollutants on the surface of the material (Atwood et al., 2017).

Different materials have been found to have different surface areas which lead to different adsorption capacities. For example, Ellass, et al. (2011) investigated the ability of Moroccan clays to remove methyl violet from aqueous solution, where the results revealed that the material had a surface area and, as a result, high adsorption capacity of 137 m<sup>2</sup>/g and 625 mg/g, respectively. Other materials with high surface areas include acid activated kaolinite, raw bentonite clay and acid bentonite clay with surface areas of 358.6 m<sup>2</sup>/g, 25.7 m<sup>2</sup>/g and 84.6 m<sup>2</sup>/g, respectively. Although surface area and pore volume of a material contributes to its adsorption capacity, the mechanisms of adsorption are also likely to be influenced by the electrostatic forces between the adsorbent and the adsorbate (Toor and Jin, 2012; Hai et al., 2015; Ngulube et al, 2016).

## **2.8 Legal requirement and water quality**

Water quality refers to chemical, physical and biological characteristics of water, usually in respect to its suitability for an intended purpose; because the quality of water that is required to wash a car is not the same quality that is required for drinking water. Water quality is usually changed and affected by human activities such as industrial dye effluents leading to dye flock on water surface, which results in less sunlight penetration for aquatic plants to photosynthesize, hence deviating water quality towards unsuitable and toxic (DWAF, 2002). Environmental legislation, National Environmental Management Act, 1998 (Act No, 107 of 1998) [NEMA 107: 1998] Section 24, stipulates that everyone has the right to live in an environment that is safe and not harmful to human health, while the National Water Act, 1998 [NWA, 1998] requires adequate safe drinking water delivery to recognized users. The water quality guideline is developed as a tool that advocates for environmental sustainability through elimination of pollution. Effluents emanating from textile and printing industries are very coloured and metalliferous (Belhouchat et al., 2016; Hao et al., 2000). As such, they need to be purified prior to discharge to the nearby environment. This will ensure compliance and adherence to stipulated water quality guidelines (Gitari et al., 2006; Gitari et al., 2008; Masindi et al., 2014a).

## **2.9 Mathematical modelling**

### **2.9.1 Modelling of CR removal and adsorption capacity**

Percentage removal and adsorption capacity of CR by calcined cryptocrystalline magnesite/Ca-bentonite clay nanocomposite were evaluated using equations (2.1) and (2.2)

$$\text{Percentage removal (\%)} = \left( \frac{C_i - C_e}{C_i} \right) \times 100 \quad (2.1)$$

$$\text{Adsorption capacity (q}_e\text{)} = \frac{(C_i - C_e)V}{m} \quad (2.2)$$

Where:  $C_i$  = initial CR concentration,  $C_e$  = equilibrium CR concentration,  $V$  = volume of solution;  $m$  = mass of the feedstock.

## 2.9.2 Adsorption Kinetics

Adsorption kinetics was evaluated using pseudo-first-order, second order kinetics and Intraparticle diffusion model by Weber Morris (Ho and McKay, 1999, Ho et al., 2000, Ho et al., 2005, Tran et al., 2017). A Lagergren pseudo first order kinetic model is a well-known model that is used to describe mechanisms of metal species adsorption by an adsorbent. It can be written as follows:

$$\log(q_e - q_t) = \log q_e - \frac{k_1 t}{2.303} \quad (2.3)$$

Where  $k_1$  ( $\text{min}^{-1}$ ) is the pseudo-first-order adsorption rate coefficient and  $q_e$  and  $q_t$  are the values of the amount adsorbed per unit mass at equilibrium and at time  $t$ , respectively. The pseudo-second-order kinetic model is another kinetic model that is widely used to describe the adsorption mechanism from an aqueous solution. The linearized form of the pseudo-second-order rate equation can be written as follow:

$$\frac{t}{q_t} = \frac{k_2 t}{k_2 q_e^2} + \frac{t}{q_e} \quad (2.4)$$

Where  $k_2$  [ $\text{g (mg min}^{-1}\text{)}$ ] is the pseudo-second-order adsorption rate coefficient and  $q_e$  and  $q_t$  are the values of the amount adsorbed per unit mass at equilibrium and at time  $t$ , respectively. The overall kinetics of the adsorption from solutions may be governed by the diffusional processes as well as by the kinetics of the surface chemical reaction. In diffusion studies, the rate is often expressed in terms of the square root time as denoted below:

$$q_t = k_{id} t^{1/2} + C_i \quad (2.5)$$

Where  $k_{id}$  ( $\text{mgg}^{-1} \text{min}^{-1/2}$ ) is the intraparticle diffusion coefficient (slope of the plot of  $q_t$  vs.  $t^{1/2}$ ) and  $C_i$  is the intraparticle diffusion rate constant. Parameters were calculated to determine whether film diffusion or intraparticle diffusion is the rate limiting step. The model suggests if the sorption mechanism is via intraparticle diffusion when a plot of  $q_t$  versus  $t^{1/2}$

will be linear; and intraparticle diffusion is the sole rate-limiting step when such a plot passes through the origin. When the sorption process is controlled by more than one mechanism, then a plot of  $qt$  versus  $t^{1/2}$  will be multi-linear (Tran et al., 2017).

### 2.9.3 Adsorption isotherms

Adsorption isotherms were evaluated using the most popular models and they include: Langmuir and Freundlich adsorption isotherms (Tran et al., 2017). Thermodynamics evaluations were done using Gibbs free energy equation (Tran et al., 2017). The most important model of monolayer adsorption was developed by Langmuir. This isotherm may be denoted by the undermentioned equation:

$$q_e = \frac{Q_0 b C_e}{1 + b C_e} \quad (2.6)$$

The constant  $Q_0$  and  $b$  are characteristics of the Langmuir equation and can be determined from a linearized form of equation 2.7. The Langmuir isotherm is valid for monolayer sorption due to a surface with finite number of identical sites and can be expressed in the following linear form:

$$\frac{C_e}{Q_e} = \frac{1}{Q_m b} + \frac{C_e}{Q_m} \quad (2.7)$$

The essential characteristics of the Langmuir isotherm can be expressed in terms of a dimensionless constant separation factor or equilibrium parameter,  $R_L$ , which can be determined by the following equation:

$$R_L = \frac{1}{1 + b C_0} \quad (2.8)$$

Where,  $C_e$  = equilibrium concentration ( $\text{mg L}^{-1}$ ),  $q_e$  = amount adsorbed at equilibrium ( $\text{mg g}^{-1}$ ),  $Q_m$  = Langmuir constants related to adsorption capacity ( $\text{mg g}^{-1}$ ) and  $b$  = Langmuir constants related to energy of adsorption ( $\text{L mg}^{-1}$ ). A plot of  $C_e$  versus  $C_e/Q_e$  should be linear if the data conforms to the Langmuir isotherm. The value of  $Q_m$  is determined from the slope and the intercept of the plot. It is used to derive the maximum adsorption capacity and  $b$  is determined from the original equation and represents the degree of adsorption.

The Freundlich adsorption isotherm describes the heterogeneous surface energy by multilayer adsorption. The Freundlich isotherm is formulated as follows:

$$q_e = kC_e^{1/n} \quad (2.9)$$

The equation may be linearized by taking the logarithm of both sides of the equation and can be expressed in linear form as follows:

$$\log q_e = n \log C_e + \log k_f \quad (2.10)$$

Where  $C_e$  = equilibrium concentration ( $\text{mg L}^{-1}$ ),  $q_e$  = amount adsorbed at equilibrium ( $\text{mg g}^{-1}$ ),  $K$  = Partition Coefficient ( $\text{mg g}^{-1}$ ) and  $n$  = degree of adsorption. A linear plot of  $\log C_e$  versus  $\log q_e$  indicates whether the data is described by the Freundlich isotherm. The value of  $K$  implies that the energy of adsorption on a homogeneous surface is independent of surface coverage and  $n$  is an adsorption constant which reveals the rate at which adsorption is taking place.

#### 2.9.4 Thermodynamic studies

In order to fully understand the nature of adsorption, the thermodynamic parameters such as free energy change ( $\Delta G$ ) can be calculated. It is possible to estimate these thermodynamic parameters for adsorption reaction by considering the equilibrium constant under the experimental conditions. The Gibbs free energy change of adsorption was calculated using the following equation:

$$\Delta G = -RT \ln K_c \quad (2.11)$$

$$\Delta G^0 = \Delta H^0 + T\Delta S^0 \quad (2.12)$$

Where,  $R$  is gas constant ( $8.314 \text{ J mg}^{-1} \text{ K}^{-1}$ ),  $T$  is temperature in Kelvin and  $K_c$  is the equilibrium constant ( $K_c = q_e/c_e$ ). The positive  $\Delta G^0$  value indicates that the sorption process is non-spontaneous in nature and requires energy input whereas the negative  $\Delta G^0$  value indicates that the reaction is spontaneous and require no energy input. The enthalpy change  $\Delta H^0$  (intercept) and entropy change  $\Delta S^0$  (slope) for adsorption processes were calculated from the plot of  $\Delta G^0$  versus  $T$  gives the intercept and slope of equation 2.12.

An error analysis was required to evaluate the fit of the adsorption isotherms to experimental data. In the present study, the linear coefficient of determination ( $R^2$ ) was employed for the error analysis. The linear coefficient of determination was calculated by using the equation 2.13:

$$r = \frac{n \sum xy - (\sum x)(\sum y)}{\sqrt{n(\sum x^2) - (\sum x)^2} \sqrt{n(\sum y^2) - (\sum y)^2}} \quad (2.13)$$

Theoretically, the  $R^2$  value varies from 0 to 1. The  $R^2$  value shows the variation of experimental data as explained by the regression equation. In most studies, the coefficient of determination,  $R^2$ , was applied to determine the relationship between the experimental data and the kinetics or isotherms.

## 2.10 Concluding remarks

This chapter briefly outlined the sources and uses of dyes related to industrial applications, as well as the impacts of the dye effluent discharged by dye industries. A detailed account about the available techniques for dyes removal is provided. The advantages and disadvantages of current dye removal techniques are summarized. Adsorption is one of the most effective techniques for dye removal. Unfortunately the use of adsorption for dye removal is restricted due to high cost and regeneration difficulties of activated carbon, which is a widely used adsorbent for industrial adsorption processes. This limitation highlights the need for low-cost adsorbents. However, it has been found that clays modifications have the potential to replace activated carbons. Clays have high potential for dye removal; however, the application of clays is confined to the treatment of basic dyes due to the presence of net negative charges on their surface. Hence, there is a need for clay modification to enhance their surface area and adsorption properties. Mechanochemically synthesized composite of magnesite and bentonite clay has mildly been used for dye remediation, and have been successfully used for removal of Congo red dye from aqueous solution in this study. This study is to explore the potential application of cryptocrystalline magnesite-calcium-bentonite clay composites for removal of Congo red dye from aqueous solution.

## CHAPTER THREE

### MATERIALS AND METHODS

#### 3.1 Sampling

Raw magnesite rocks were collected from the Folovhodwe Magnesite Mine in Limpopo Province, South Africa, without any prior processing. Bentonite clay was supplied by ECCA (Pty) Ltd (Cape Town, South Africa). Dyes effluent was collected from a printing industry in Pretoria.

#### 3.2 Preparation of the feed materials

Magnesite rock samples were milled to a fine powder (Retsch RS 200 mill) and sieved (32  $\mu\text{m}$  particle sizes). The ball milled cryptocrystalline magnesite powder was calcined at  $\geq 900^\circ\text{C}$  as reported in literature (Birchal et al., 2000, Sasaki and Moriyama, 2014). Raw bentonite clay was washed and soaked in ultra-pure water (18.2  $\text{M}\Omega\text{-cm}$ ) and drained after 10 minutes. The washing bentonite clay was done in a way that the ultrapure water covered the whole material in a beaker, with the water allowed to overflow. In order to gain assurance of total removal of impurities from the clay, repetition of the procedure was done four times. The washed bentonite clay was then dried for 24 hrs at  $105^\circ\text{C}$  in an oven. After drying, the samples were ball milled into a fine powder using Retsch RS 200 mill. To maintain uniformity, the milled samples were sieved through a 32  $\mu\text{m}$  particle size sieves to obtain the required particle sizes with the desired reactivity.

#### 3.3 Synthesis of the clay-based-nanocomposite

In this study, calcined cryptocrystalline magnesite/Ca-bentonite clay nanocomposite was mechanochemically synthesized by a vibratory ball mill as described by Masindi et al. (2017). The nanocomposite was prepared by mixing using a horizontal shaker where powdered bentonite clay (500g) and calcined magnesite (500g) were mixed at a mass ratio of 1:1 wt%. The mixture was crushed and homogenised by pulverizing into a fine powder (Retsch RS 200 mill) at 1600 rpm for 30 minutes using a vibratory ball miller. Thereafter, the newly fabricated composite was sieved through  $\leq 32 \mu\text{m}$  particle size sieves. The sieved materials were kept in sealed zip-lock plastic bags until use.

### **3.4 Characterization of feed and recovered materials**

#### **3.4.1 Mineralogical composition**

X-ray diffraction patterns (XRD) were obtained from a PANalytical X'Pert Pro powder diffractometer using Cu-K $\alpha$  radiation with X'Celerator detector. A step size of 0.02° and scan speed of 0.03° per second were used to conduct XRD patterns taken at high angles of  $2\theta \approx 10 - 90^\circ$ . A back loading preparation method was used to prepare samples for the feed material and products. X'Pert Highscore plus software was used to identify phases in the materials, with the relative phase amounts (mass%) estimated by Rietveld quantitative analysis which is a powerful method for determining the quantities of crystalline and amorphous components in multiphase mixtures (Hiller, 2013).

#### **3.4.2 Morphological analysis**

To obtain information on morphologies and size distribution of the solid materials, a JEOL JSM7500 microscope was used to collect high-vacuum scanning electron micrographs (SEM images). Samples were dispersed on a carbon tape and sputter-coated with a thin, conductive layer of gold using an Emitech K950X sputter coater, with the acceleration voltage being 2.00 kV. Energy Dispersive X-Ray Analysis (EDX), also referred to as EDS, is an x-ray technique used to evaluate the elemental composition of materials. The EDX system used was attached to an SEM instrument (FIB-SEM, Auriga from Carl Zeiss), where the imaging capability of the microscope identified the specimen of interest.

### **3.5 Batch experimental studies**

The adsorption of CR by bentonite clay, pre-treated magnesite, and their nanocomposite were tested in batch experiments. A shaker was used for mixing the solution. To establish the optimum conditions that are suitable for the removal of Congo Red (CR), several operational parameters were optimized and they include effects of contact time, adsorbent dosage, CR concentration, solution pH and temperature. To ensure validity of the results and repeatability, all experiments were performed in triplicate and the data was reported as average values.

#### **3.5.1 Effect of contact time**

Volumes (100 mL) of 10 mg/L CR were pipetted into 9, 250 mL containers. 1 g of respective adsorbent sample was added into each container. The mixtures were then equilibrated for 1, 5, 10, 15, 20, 25, 30, 45 and 60 minutes at 250 rpm using the shaker. The colour removal of

CR dye solutions was analysed by measuring the absorbance with a UV/Vis spectrophotometer (Shimadzu UV- 2450) at  $\lambda_{\text{max}} = 614 \text{ nm}$ .

### 3.5.2 Effect of dosage

Volumes (100 mL) of 10 mg/L CR were pipetted into 7, 250 mL containers and varying masses (0.1, 0.5, 1, 2, 3, 4, and 5 g) of the respective adsorbent were added into each flask, respectively. The mixtures were agitated using a shaker for an optimum time of 30 min at 250 rpm. The CR content was determined as described in the preceding section.

### 3.5.3 Effect of species concentration

To investigate the effects of adsorbate concentration on reaction kinetics, several dilutions were made from the simulated CR stock solution. The capacity of the adsorbent to remove CR from aqueous solution was assessed by varying the CR concentrations. Solutions ranging from 1, 5, 10, 20, 40, 80, and 120 mg/L of CR were prepared into individual containers. One (1) g of the composite was added to each container. The mixtures were equilibrated for 30 minutes using a horizontal shaker. The CR content was determined as described in 3.5.1. Standard CR dye solution concentration using UV-VIS spectroscopy is shown in **Figure 3.1**.

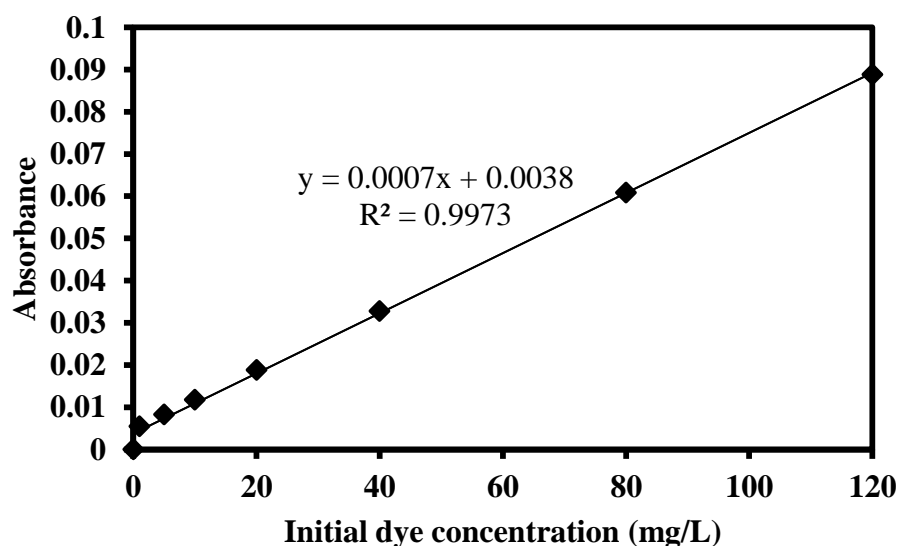


**Figure 3.1:** Standard CR dye solution concentration using UV-VIS spectroscopy

### 3.5.4 Effect of solution pH

Ten 100 mL with 10 mg/L of CR were pipetted into 250 mL containers and the pH of the solution was adjusted from 1, 2, 3, 4, 5, 6, 7, 8, 9, and 10. One (1) g of the respective adsorbent was added into each container. The mixtures were agitated using a shaker for 30 mins at 250 rpm. The pH was determined using CRISON pH meter. CR contents were determined as described in 3.5.1.

### 3.5.5 Effect of temperature

Four (4) 100 mL with 10 mg/L of CR were pipetted into 250 mL containers. One (1) g of the respective was added into each container. The mixtures were agitated using a shaker for an optimum time of 30 mins at 250 rpm. Temperature was monitored using a Thermometer in a range of 25, 40, 50, 60, and 70°C. The CR content was determined as described in 3.5.1.

## 3.6 Removal of CR at optimized conditions

Congo Red (CR) effluent emanating from a printing company in Pretoria was treated at established optimized conditions in order to assess the effectiveness of bentonite clay, pre-treated magnesite, and their nanocomposite. The CR contents were determined as described previously.

## 3.7 Desorption and regeneration studies

Desorption and regeneration gives useful insights about the possibility of reusing the adsorbent. In this study, desorption evaluations were done using methanol, ethanol, butanol, acetone and water at 10 minutes of equilibration using a shaker. Thereafter, methanol was used for desorption and the cycles were repeated 10 times.

## 3.8 Computation of CR % removal and adsorption capacity

The percentage removal and adsorption capacity of CR by bentonite clay, pre-treated magnesite, and their nanocomposite were evaluated using equation (3.1) and (3.2):

$$\text{Percentage removal (\%)} = \left( \frac{C_i - C_e}{C_i} \right) \times 100 \quad (3.1)$$

$$\text{Adsorption capacity (q}_e\text{)} = \frac{(C_i - C_e)V}{m} \quad (3.2)$$

Where:  $C_i$  = initial CR concentration,  $C_e$  = equilibrium CR concentration,  $V$  = volume of solution;  $m$  = mass of the feedstock.

### 3.9 Adsorption Kinetics

Adsorption kinetics was evaluated using pseudo-first-order, and second order kinetics (Ho and McKay, 1999, Ho et al., 2000, Ho et al., 2005, Tran et al., 2017).

#### 3.9.1 Pseudo-first-order kinetic

A Lagergren pseudo first order kinetic model is a well-known model that is used to describe mechanisms of metal species adsorption by an adsorbent. It can be written as follows (Lagergren, 1898):

$$\log(q_e - q_t) = -\frac{k_1 t}{2.303} + \log q_e \quad (3.3)$$

Where  $k_1$  ( $\text{min}^{-1}$ ) is the pseudo-first-order adsorption rate coefficient and  $q_e$  and  $q_t$  are the values of the amount adsorbed per unit mass at equilibrium and at time  $t$ , respectively.

#### 3.9.2 Pseudo-second-order kinetic

Pseudo-second-order kinetic model is another kinetic model that is widely used to describe the adsorption mechanism from an aqueous solution. The linearized form of the pseudo-second-order rate equation can be written as follows (Ho and McKay, 1999):

$$\frac{t}{q_t} = -(k_2 q_e) q_t + k_2 q_e^2 \quad (3.4)$$

Where  $k_2$  [ $\text{g} (\text{mg min}^{-1})$ ] is the pseudo-second-order adsorption rate coefficient and  $q_e$  and  $q_t$  are the values of the amount adsorbed per unit mass at equilibrium and at time  $t$ , respectively.

### 3.10 Adsorption isotherms

Adsorption isotherms were evaluated using the most popular models and they include: Langmuir and Freundlich adsorption isotherms (Lima, 2015, Tran et al., 2017).

#### 3.10.1 Langmuir adsorption isotherm

The most important model of monolayer adsorption was developed by Langmuir. This isotherm may be denoted by the undermentioned equation:

$$q_e = \frac{Q_0 b C_e}{1 + b C_e} \quad (3.5)$$

The constant  $Q_0$  and  $b$  are characteristics of the Langmuir equation and can be determined from a linearized form of equation 6. The Langmuir isotherm is valid for monolayer sorption due to a surface with finite number of identical sites and can be expressed in the following linear form (Langmuir, 1916):

$$\frac{C_e}{Q_e} = \frac{1}{Q_m b} + \frac{C_e}{Q_m} \quad (3.6)$$

The essential characteristics of the Langmuir isotherm can be expressed in terms of a dimensionless constant separation factor or equilibrium parameter,  $R_L$ , which can be determined by the following equation:

$$R_L = \frac{1}{1 + bC_0} \quad (3.7)$$

Where,  $C_e$  = equilibrium concentration ( $\text{mg L}^{-1}$ ),  $q_e$  = amount adsorbed at equilibrium ( $\text{mg g}^{-1}$ ),  $q_m$  = Langmuir constants related to adsorption capacity ( $\text{mg g}^{-1}$ ) and  $b$  = Langmuir constants related to energy of adsorption ( $\text{L mg}^{-1}$ ). A plot of  $C_e$  versus  $C_e/Q_e$  should be linear if the data conforms to the Langmuir isotherm. The value of  $Q_m$  is determined from the slope and the intercept of the plot. It is used to derive the maximum adsorption capacity and  $b$  is determined from the original equation and represents the degree of adsorption.

### 3.10.2 Freundlich adsorption isotherm

The Freundlich adsorption isotherm describes the heterogeneous surface energy by multilayer adsorption. The Freundlich isotherm is formulated as follows:

$$q_e = kC_e^{1/n} \quad (3.8)$$

The equation may be linearized by taking the logarithm of both sides of the equation and can be expressed in linear form as follows (Freundlich, 1906):

$$\log q_e = n \log C_e + \log k_f \quad (3.9)$$

Where  $C_e$  = equilibrium concentration ( $\text{mg L}^{-1}$ ),  $q_e$  = amount adsorbed at equilibrium ( $\text{mg g}^{-1}$ ),  $K$  = Partition Coefficient ( $\text{mg g}^{-1}$ ) and  $n$  = degree of adsorption. A linear plot of  $\log C_e$  versus  $\log q_e$  indicates whether the data is described by the Freundlich isotherm. The value of  $K$  implies that the energy of adsorption on a homogeneous surface is independent of

surface coverage and  $n$  is an adsorption constant which reveals the rate at which adsorption is taking place.

### 3.11 Adsorption thermodynamics

The thermodynamic study was carried out to reveal the nature of the adsorption of CR onto bentonite clay, pre-treated magnesite, and their nanocomposite. The thermodynamic parameters, such as the Gibbs energy change ( $\Delta G^0$ ) ( $\text{J mol}^{-1}$ ), the enthalpy change ( $\Delta H^0$ ) ( $\text{J mol}^{-1}$ ) and the entropy change ( $\Delta S^0$ ) ( $\text{J.K}^{-1} \text{ mol}^{-1}$ ) were determined using the following equation:

$$K_L = \frac{q_e}{C_e} \quad (3.10)$$

$$\Delta G^0 = \Delta H^0 - T\Delta S^0 \quad (3.11)$$

$$\Delta G^0 = RT \ln K_L \quad (3.12)$$

Equation 13 is obtained from Equations 3.11 and 3.12.

$$\ln K_L = \frac{\Delta S^0}{R} - \frac{\Delta H^0}{R} \cdot \frac{1}{T} \quad (3.13)$$

Where,  $R$  is the universal gas constant ( $8.314 \text{ J K}^{-1} \text{ mol}^{-1}$ ),  $T$  is the absolute temperature in Kelvin and  $K_L$  is the distribution equilibrium constant (dimensionless). By plotting a graph of  $\ln(K_L)$  versus  $1/T$ , a straight line is obtained. From the intercept and slope of the plot, it is possible to calculate the changes in Entropy  $\Delta S^0$  and changes in enthalpy ( $\Delta H^0$ ), respectively.

### 3.12 Desorption study

The amount of CR desorbed from the matrices of bentonite clay, pre-treated magnesite, and their nanocomposite is calculated using the following equation (Vu et al., 2018):

$$\% \text{Desorption} = \frac{q_e}{q_e} - \frac{q_r}{q_d} \times 100 \quad (3.14)$$

Where  $q_r$  (mg/g) is the mass of CR dye that remained adsorbed at the end of the desorption process,  $q_d$  (mg/g) is the mass of CR dye desorbed if the adsorption was reversible.

### 3.13 Determination of Point of Zero Charge (PZC)

The pH for point of zero charge ( $pH_{ZPC}$ ) of bentonite clay, pre-treated magnesite and their composite were determined using solid addition method as described by Masindi and Gitari (2013). Forty (40) mL of 0.1 M KCl was transferred to a series of 100 mL bottles. The initial pH ( $pH_{initial}$ ) of the solutions was adjusted between the range of 2 -13 by adding 0.1 M HCl and 0.1 M NaOH solutions. The total volume of the solution in each tube was adjusted exactly to 50 ml by adding 0.1 M KCl. Furthermore, 0.5 g of the ball milled and calcined magnesite was added to all tubes and the suspensions were then equilibrated for 48 hrs. After equilibration, the solution was filtered and the final pH values ( $pH_{final}$ ) of the filtrate were measured again. The difference between initial and final pH ( $pH_f$ ) values ( $\Delta pH = pH_i - pH_f$ ) was plotted against  $pH_i$ . The point of intersection of the resulting curve with abscissa, at which  $\Delta pH=0$ , was taken as the point of zero charge.

## CHAPTER FOUR

### RESULTS AND DISCUSSIONS

This chapter seeks to report the results obtained in this study and duly discuss them. It will also point out the mechanisms that are governing the removal of Congo Red (CR) from aqueous solution using bentonite clay, pre-treated magnesite and their composite.

#### 4.1 Characterisation

##### 4.1.1 Mineralogical analysis

The mineralogical characteristics of bentonite clay, pre-treated magnesite, and their nanocomposite are shown in **Figure 4.1**.

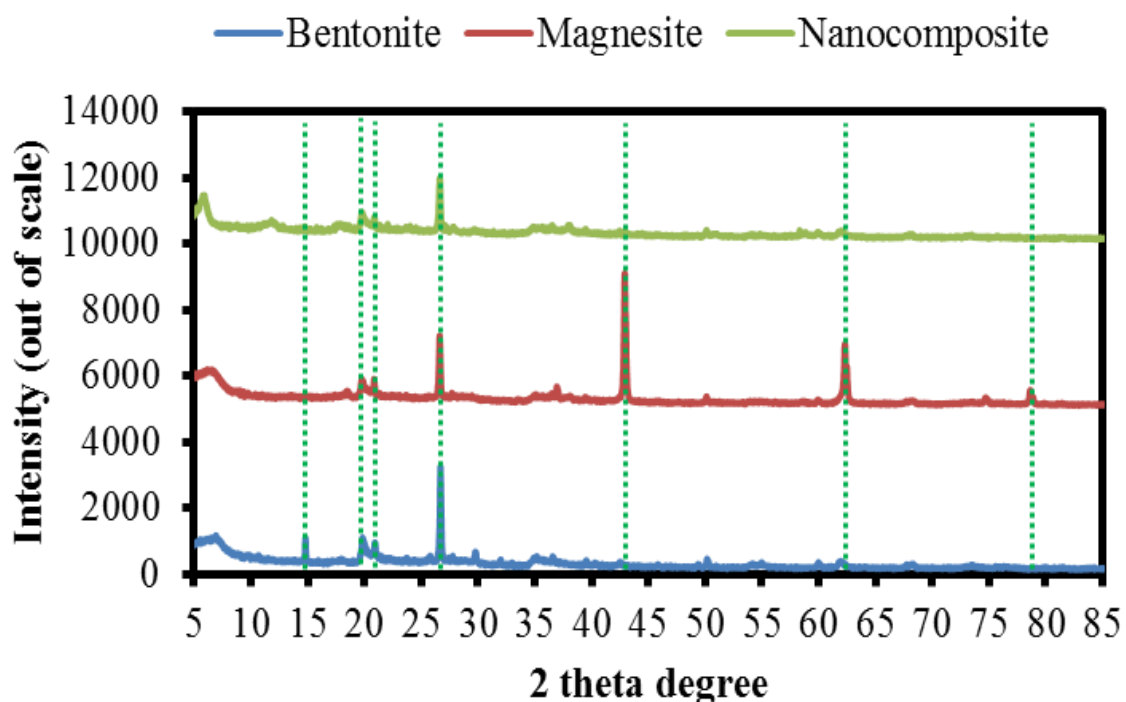


**Figure 4.1:** Mineralogical characteristics of bentonite clay, pre-treated magnesite, and their nanocomposite

As shown in **Figure 4.1**, bentonite clay was observed to contain muscovite, quartz, and montmorillonite at 15, 20, and 26  $\theta$  degrees. Pre-treated magnesite was determined to contain quartz (20), periclase (26), and magnesite (43 and 62) 2 theta degrees respectively. Their nanocomposite was observed to contain quartz as a crystalline phase. The other

materials were observed to have disappeared. This may be attributed to calcination and vibratory ball milling that leads to a break in the material structures hence the amorphous nature.

#### 4.1.2 Morphological analysis

The morphological characteristics of bentonite clay, pre-treated magnesite, and their nanocomposite are shown in **Figure 4.2**.

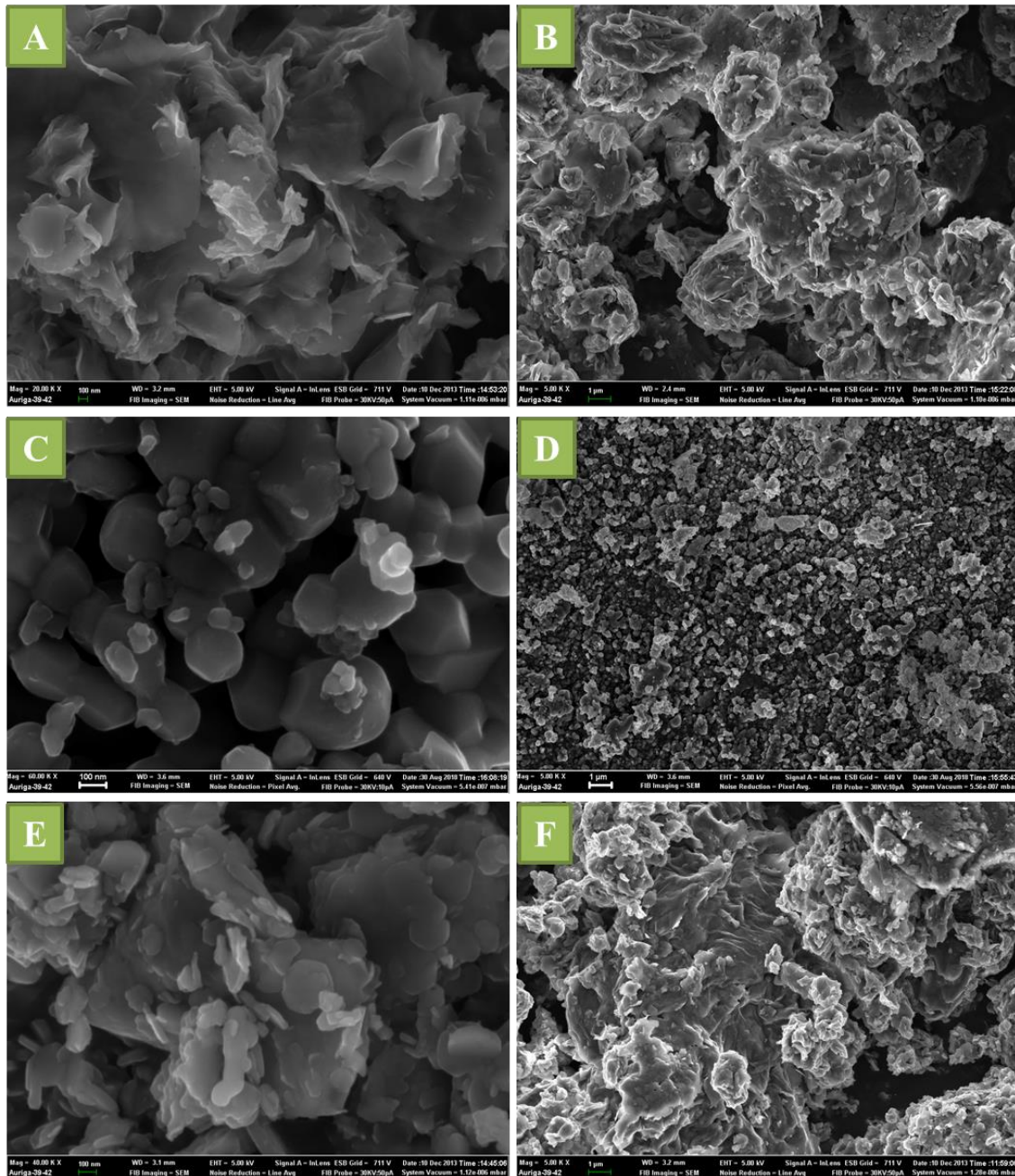


**Figure 4.2:** Morphological characteristics of bentonite clay, pre-treated magnesite, and their nanocomposite

As shown in **Figure 4.2**, bentonite clay depicted flower-like and leafy structures on its surfaces. Pre-treated magnesite was determined to contain nanosheets of octagonal structures with varying sizes. Their nanocomposite was observed to contain a sandwich of both minerals. Leafy structures mixed with sheet-like-structures were also observed to be present.

## 4.2 Batch adsorption experiments

The performance appraisal for the removal of Congo Red (CR) using bentonite clay, pre-treated magnesite, and their nanocomposite are explored as shown in **Figures** below.

### 4.2.1 Effect of contact time

Variations on the removal of CR dye from aqueous solution using bentonite clay, pre-treated magnesite, and their nanocomposite as a function of contact time is shown in **Figure 4.3**.

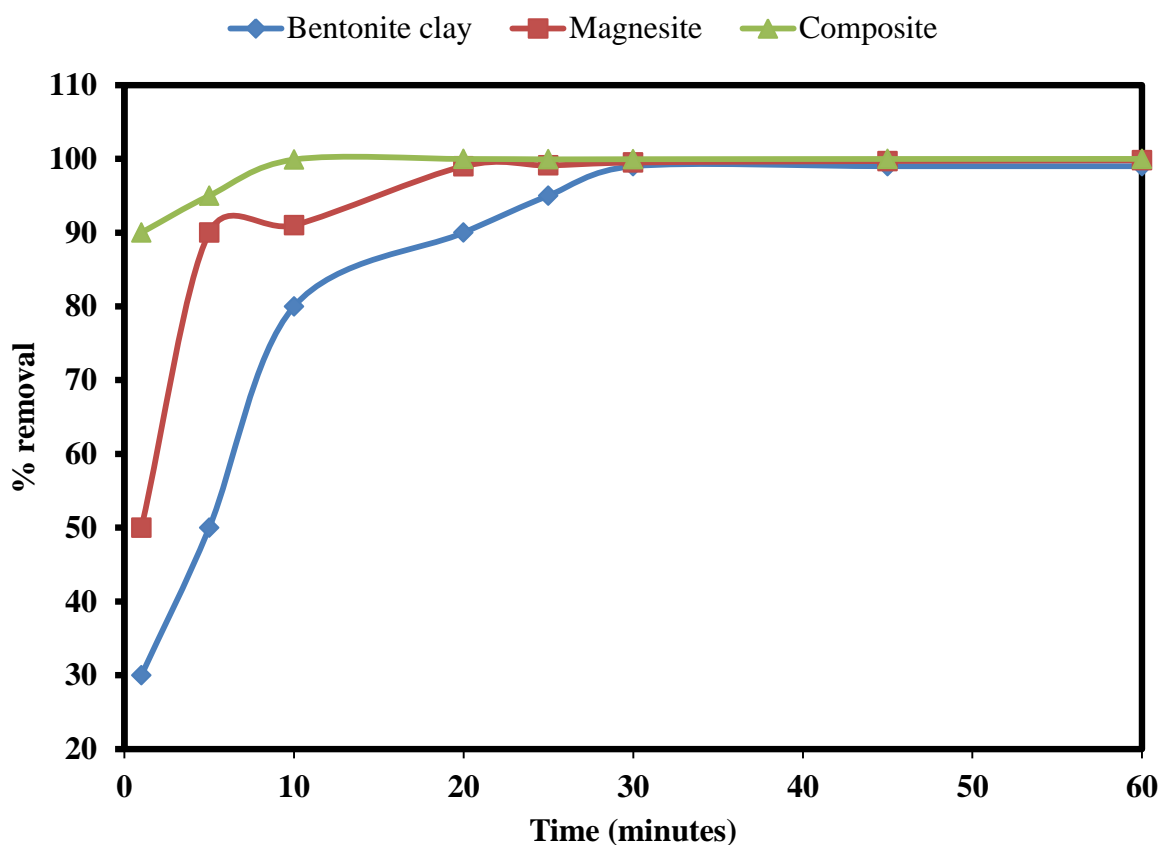


**Figure 4.3:** Variations in percentage removal of CR as a function of contact time (conditions: 1g, 10 mg/L, 250 rpm, pH = 7 and room temperature).

As shown in **Figure 4.3**, the removal of CR dye by the nanocomposite was observed to increase with an increase in contact time. For bentonite clay, the removal of CR was observed

to increase with time from 0 to 30 minutes. Thereafter, no significant change was observed hence depicting that the material is saturated with the adsorbate. For pre-treated magnesite, the removal of CR was observed to increase with time from 0 to 20 minutes. Thereafter, no significant change was observed hence depicting that the material is saturated with the adsorbate. For their nanocomposite, the removal of CR was observed to be rapid from 1 to 10 minutes of shaking. Thereafter, there was no increase in percentage removal of CR that was observed hence depicting a system that has reached equilibrium. This may be attributed to a rapid uptake of CR or a depletion of CR from an aqueous system. From the obtained results, 20 minutes were taken as optimum shaking time for subsequent experiments. This was chosen because a system requires enough time to deplete the pollutants from water.

#### 4.2.2 Effect of adsorbent dosage

Variations on the removal of CR dye from aqueous solution using bentonite clay, pre-treated magnesite, and their nanocomposite as a function of dosage is shown in **Figure 4.4**.

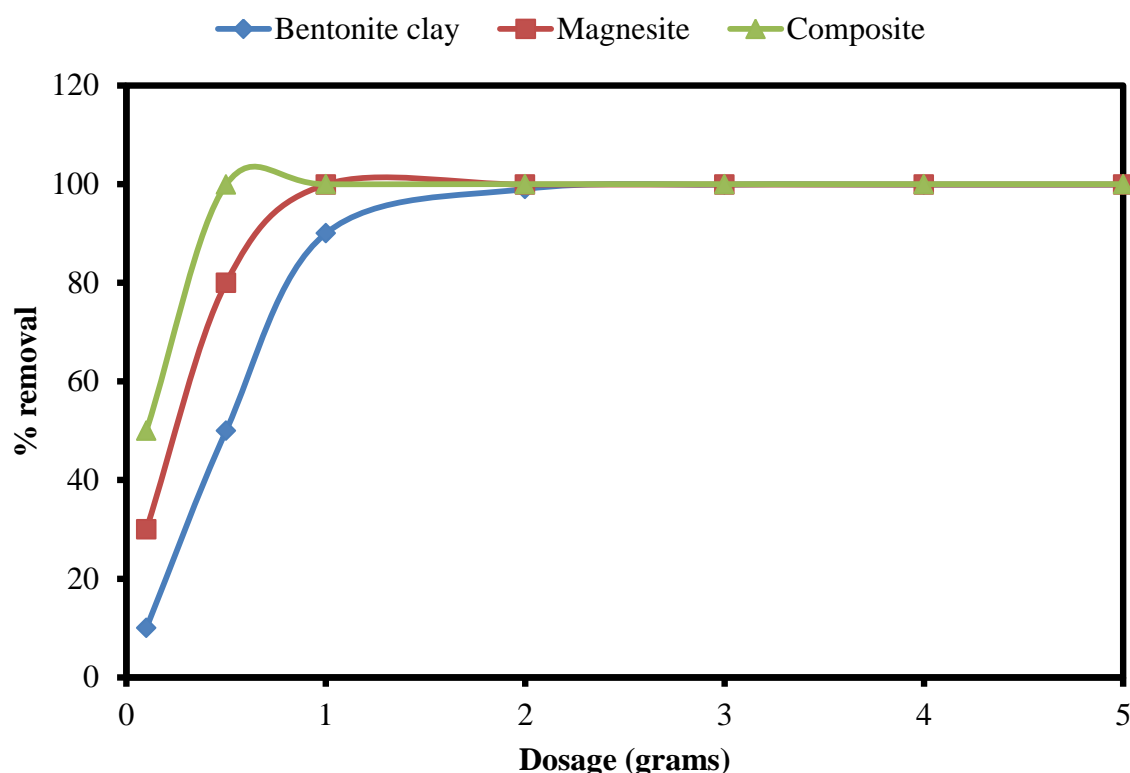


**Figure 4.4:** Variations in percentage removal of CR as a function of dosage (conditions: 20 minutes of mixing, 10 mg/L, 250 rpm, pH = 7 and room temperature).

As shown in **Figure 4.4**, there was an increase in CR dye removal which was observed with an increase in the adsorbent dosage. This may be attributed to an increase in adsorption sites as the dosage increases hence increase the performance of the material. For bentonite clay, there was a rapid increase in percentage removal of from 0.1 to 2 g, thereafter, no significant change was observed. For pre-treated magnesite, a rapid uptake of CR was observed between 0.1 to 1 g of the adsorbent. Thereafter, no significant change was observed hence depicting that the reaction has reached equilibrium. For their nanocomposite, there was a rapid uptake of CR from 0.1 g to 0.5 g. Thereafter, it commenced to flatten up hence indicating that the adsorption has reached equilibrium. As such, it was noted that 0.5 g of the nanocomposite was sufficient for the removal of 10 mg/L of CR from aqueous solution and it will be used for subsequent experiments.

#### 4.2.3 Effect of CR concentration

Variations on the removal of CR dye from aqueous solution using bentonite clay, pre-treated magnesite, and their nanocomposite as a function of CR concentration is shown in **Figure 4.5**.

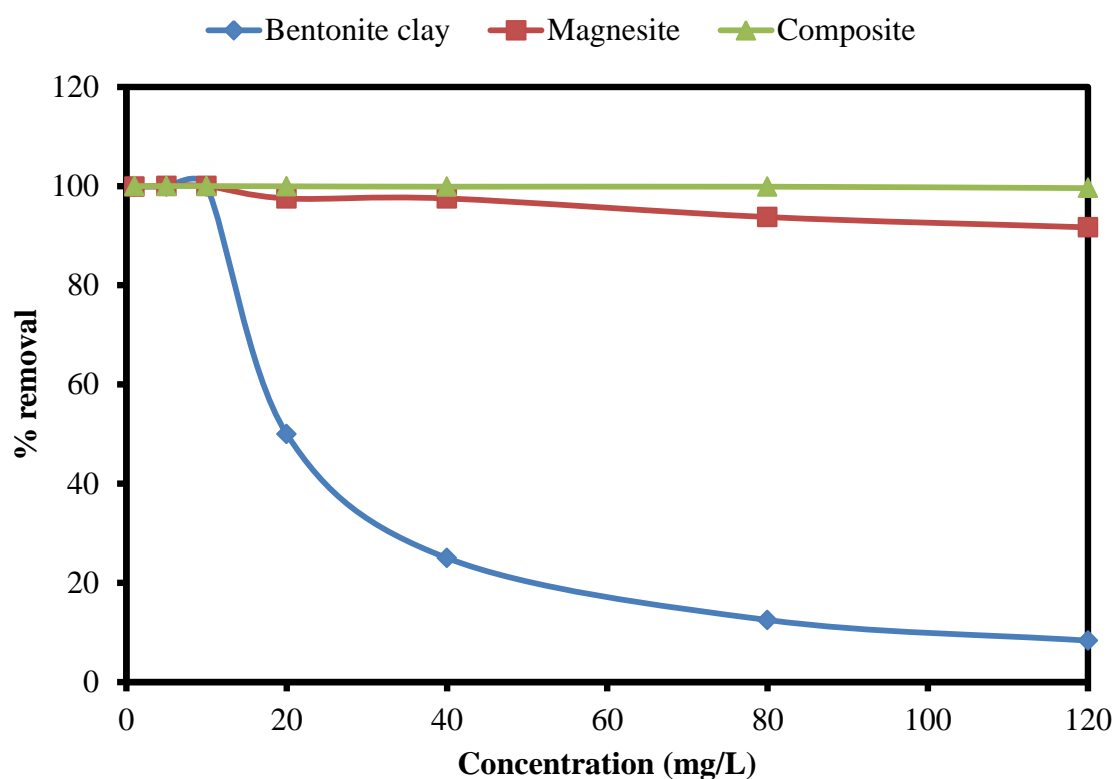


**Figure 4.5:** Variations in percentage removal of CR as a function of adsorbate concentration (conditions: 20 minutes of mixing, 0.5 g of dosage, 250 rpm, pH = 7 and room temperature).

As it can be seen in **Figure 4.5**, there was a decrease in the removal efficacy of CR with an increase in CR concentration. This may be explained by saturation of adsorbents as adsorbates concentration increases. For bentonite clay, the removal of CR was optimum from 0.1 to 10 mg/L, thereafter, it was observed to decrease with an increase in concentration. For pre-treated magnesite, there was a gradual decrease in removal efficacy with an increase in adsorbate concentration. This may be attributed to enrichment of waterbodies with  $Mg^{2+}$  that captures the anionic part of the dye. However, from 0.1 to 40 mg/L the removal efficacy was  $> 99\%$ . For their nanocomposite, the removal efficacy was observed to  $> 99\%$  from 0.1 to 120 mg/L. However, it was observed to commence to decrease beyond 120 mg/L hence depicting that the material is saturated. In that regard, 120 mg/L was taken as the optimum concentration for successive experiments.

#### 4.2.4 Effect of solution pH and the point of zero charge

Variations on the removal of CR dye from aqueous solution using bentonite clay, pre-treated magnesite, and their nanocomposite as a function of initial pH is shown in **Figure 4.6**.

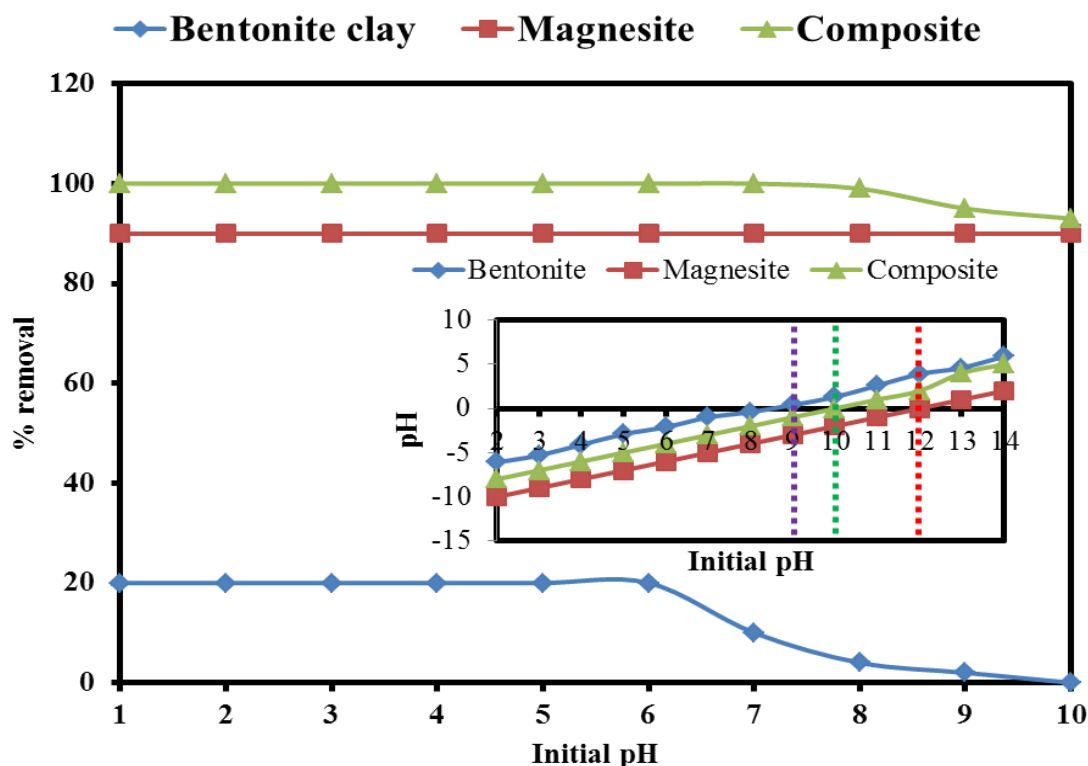


**Figure 4.6:** Variations in percentage removal of CR as a function of pH (conditions: 20 minutes, 1g of dosage, 120 mg/L, 250 rpm, and room temperature).

As shown in **Figure 4.6**, the removal of CR from aqueous solution was observed to be dependent on pH. For bentonite clay, the removal of CR was observed to decrease with an increase in pH. From pH 1 to 6, the efficacy was stable but it commenced to decrease from 7 onwards. This is directly proportional to the PZC which demonstrated that bentonite clay will be able to adsorb anions from pH 1 to 9 and then repel them post pH 9. Pre-treated magnesite was observed to be independent of pH under study, thus depicting that it can remove CR from pH 1 to 10. For their nanocomposite, the removal efficacy was observed to pH 1 to 8, thereafter, it was observed to decrease. This may also be explained by the PZC which is  $> 10$  for their nanocomposite. This indicates that below pH 10, the effectiveness of the synthesized nanocomposite is very high but it commences to depreciate post pH 10 due to repulsion forces. As such, it was concluded that the pH from 1 to 10 is suitable for the removal of CR from aqueous solution.

#### 4.2.5 Effect of temperature

Variations on the removal of CR dye from aqueous solution using bentonite clay, pre-treated magnesite, and their nanocomposite as a function of temperature is shown in **Figure 4.7**.

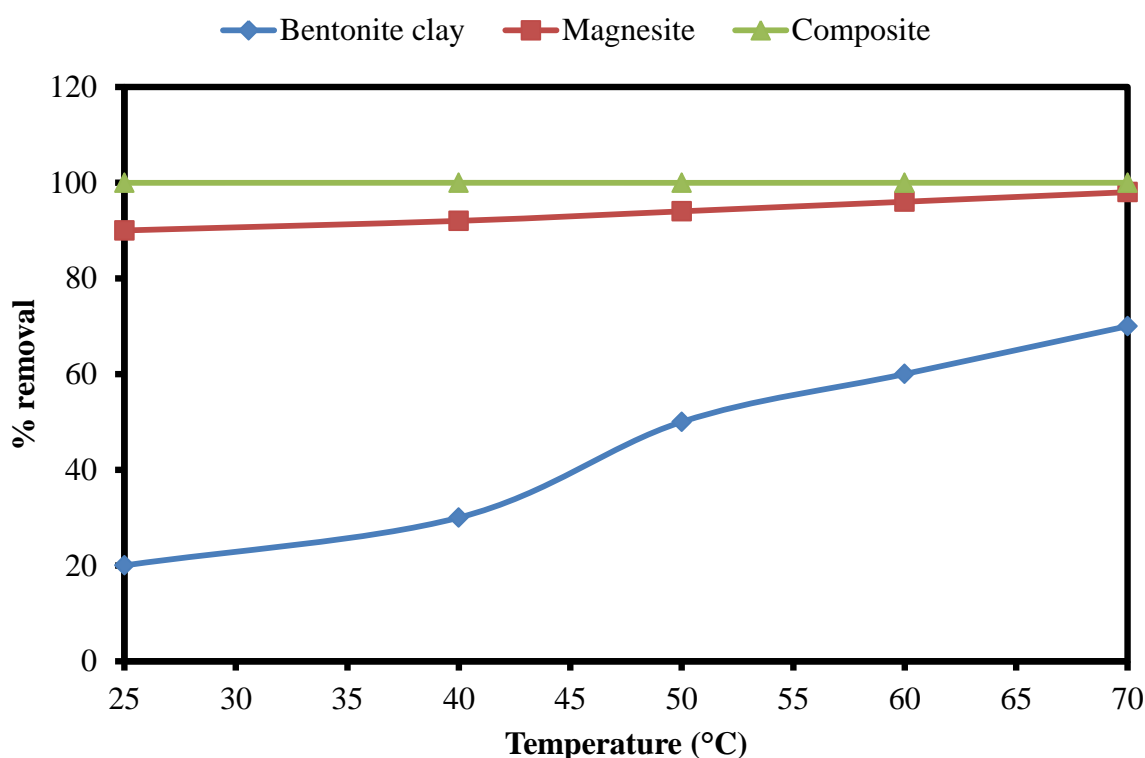


**Figure 4.7:** Variations in percentage removal of CR as a function of temperature (conditions: 20 minutes, 0.5 g of dosage, 120 mg/L, 250 rpm, and pH = 7).

As shown in **Figure 4.7**, the removal of CR from aqueous solution was observed to increase with an increase in temperature for bentonite clay, pre-treated magnesite, and their nanocomposite. For bentonite clay, the CR removal efficacy was observed to be dependent on temperature in increase from 20% at 25 °C to 70% at 70 °C. For pre-treated magnesite, it was observed to gradually increase with an increase in temperature. This may be explained by a rapid dissolution of  $Mg^{2+}$  into solution with an increase in temperature hence positively impacting the removal efficacy of CR from aqueous solution. The removal efficacy was observed to increase from 90% at 25 °C to 99% at 70 °C. For the synthesized nanocomposite, the removal efficacy was observed to be independent of temperature. The removal efficacy was very high (>99%) for all temperature gradients. As such, room temperature was taken as the optimum temperature for the nanocomposite. This will also make this technology cheap and environmental friendly.

### 4.3 Adsorption kinetics

#### 4.3.1 Pseudo-first-order kinetic

Pseudo-first-order kinetic for the adsorption of CR using bentonite clay, pre-treated magnesite, and their nanocomposite is shown in **Figure 4.8**.

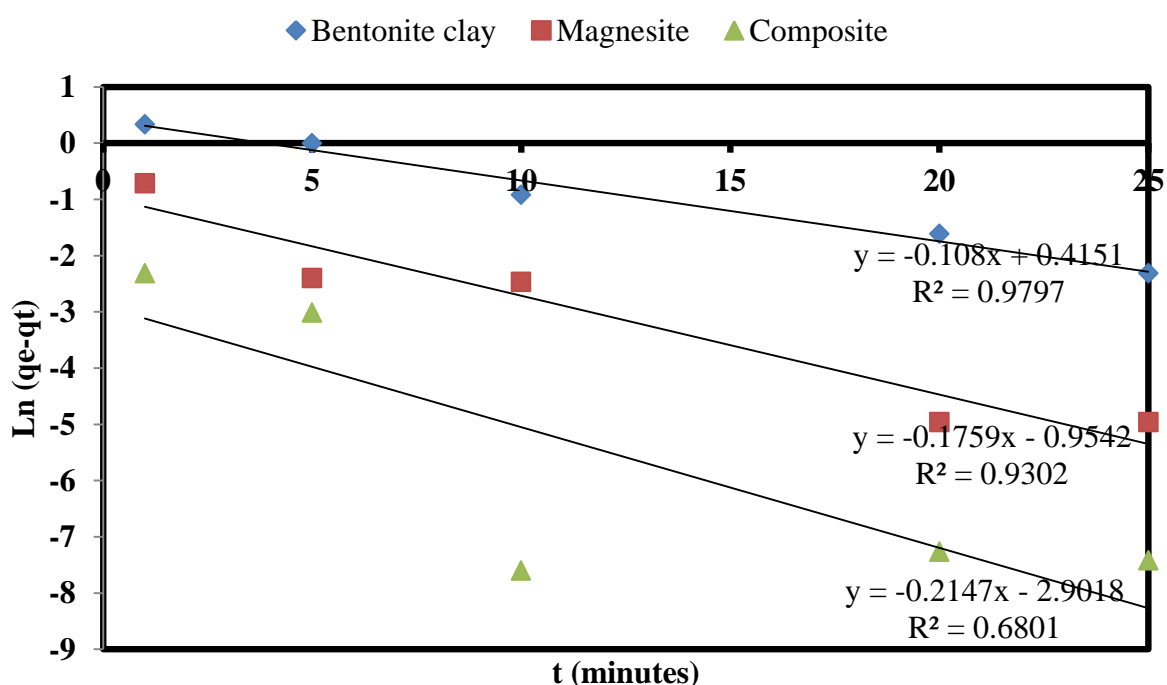


**Figure 4.8:** Pseudo-first-order kinetic for the adsorption of CR dye using bentonite clay, pre-treated magnesite, and their nanocomposite

### 4.3.2 Pseudo-second-order kinetic

Pseudo-second-order kinetic for the adsorption of CR using bentonite clay, pre-treated magnesite, and their nanocomposite is shown in **Figure 4.9**.

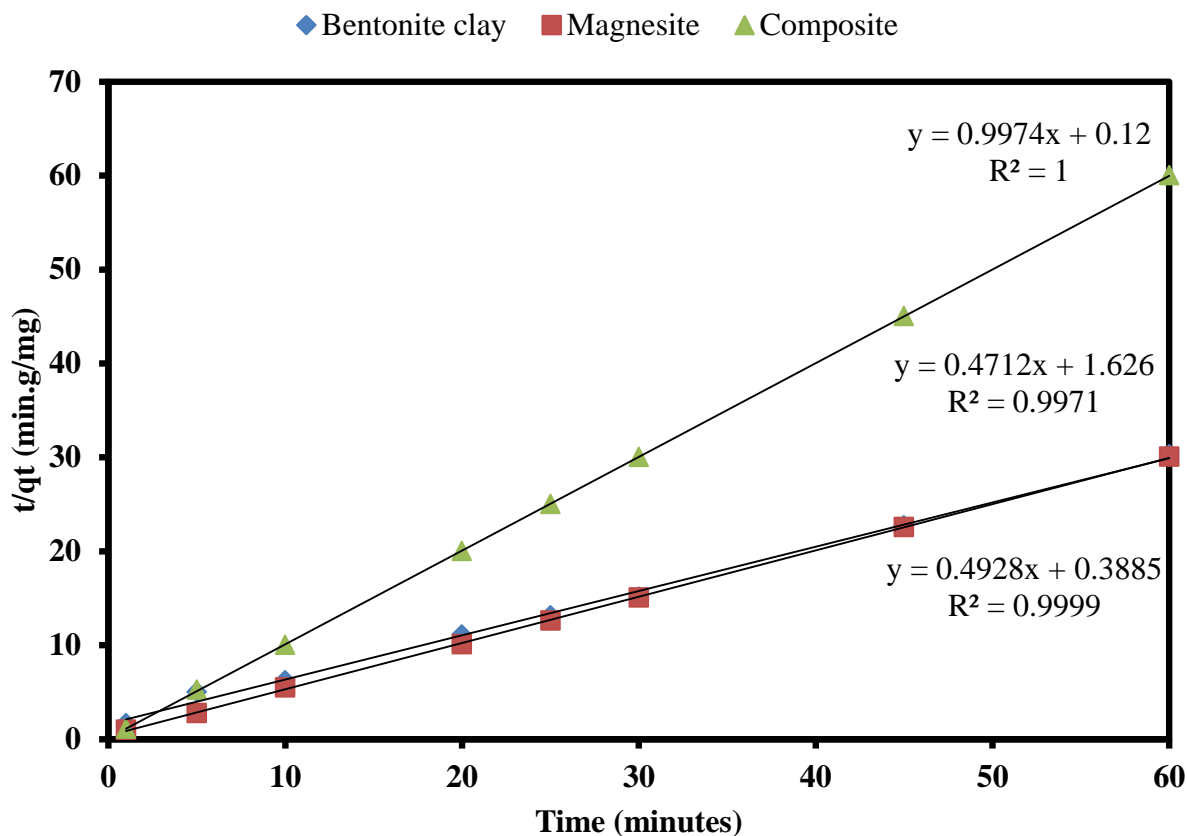


**Figure 4.9:** Pseudo-second-order kinetics for the adsorption of CR dye using bentonite clay, pre-treated magnesite, and their nanocomposite.

As shown in **Figure 4.8 and 4.9**, the removal of CR dye using bentonite clay, pre-treated magnesite, and their nanocomposite fitted very well to pseudo-second-order kinetics than pseudo-first-order kinetics for all adsorbents. This is an indication that the removal of CR using the identified adsorbents follows pseudo-second-order kinetics. Pseudo-first-order and second-order kinetic models parameters for the adsorption of CR onto bentonite clay, pre-treated magnesite, and their nanocomposite are also shown in **Table 4.1**.

**Table 4.1:** Pseudo-first-order and second-order kinetic models parameters for the adsorption of CR onto bentonite clay, pre-treated magnesite, and their nanocomposite

Adsorbent	Pseudo-first-order kinetic			Pseudo-second-order kinetic		
	$K_1$ ( $\text{min}^{-1}$ )	$q_e$ (mg/g)	$R^2$	$K_2$ (mg/g.min)	$q_e$ (mg/g)	$R^2$
Bentonite	0.48	2.6	0.98	0.6	0.8	1
Magnesite	-0.076	0.11	0.93	0.1	3.5	0.99
Composite	-0.093	$1.25 \times 10^{-3}$	0.68	8.3	0.12	0.99

The K values of pseudo-second-order kinetic were observed to be higher than those for first order kinetics hence depicting high adsorption rate for second-order kinetics. The regression analysis was observed to be 1, 0.9, and 0.9 for bentonite clay, pre-treated magnesite, and their nanocomposite respectively.

#### 4.3.3 Intra-particle diffusion model

Intra-particle diffusion model parameters for the adsorption of CR onto bentonite clay, pre-treated magnesite, and their nanocomposite are shown in **Table 4.2**.

**Table 4.2:** Intra-particle diffusion model parameters for the adsorption of CR onto bentonite clay, pre-treated magnesite, and their nanocomposite

Adsorbent	Intra-particle diffusion (Stage 1)			Intra-particle diffusion (Stage 2)		
	$K_{ip1}$	$C_1$	$R^2$	$K_{ip2}$	$C_2$	$R^2$
Bentonite	0.05	0.85	0.99	0.045	1.66	0.59
Magnesite	0.39	0.7	0.83	0.005	1.96	0.88
Composite	0.45	0.09	0.96	0.0002	0.998	0.95

As shown in **Table 4.2**, the co-ordinate was observed to be less for stage one as compared to stage two hence depicting that the dominant stage is intra-particle diffusion. The smaller value of C and  $K_{id}$  indicates that the thickness layer of the boundary is small and the intra-particle diffusion rate is very slow as shown by the low value. From the plot of  $qt$  versus  $t^{1/2}$  in **Figure 4.8**, it can be seen that the CR adsorption process depicted more than one kinetic step. The first step demonstrates the transportation of CR ions from solution to adsorbent surface which is also known as external diffusion. The second step depicted equilibrium for magnesite and its composite whereas it was increasing for bentonite clay. Moreover, the

values of  $K_{id}$  did not pass through the origin hence depicting that the CR attenuation is governed by numerous mechanisms. From the results, it can be concluded that both external and internal diffusion are governing the removal of CR ions from an aqueous system. Intra-particle diffusion model for the adsorption of CR from aqueous solution using bentonite clay, pre-treated magnesite, and their nanocomposite is shown in **Figure 4.10**.

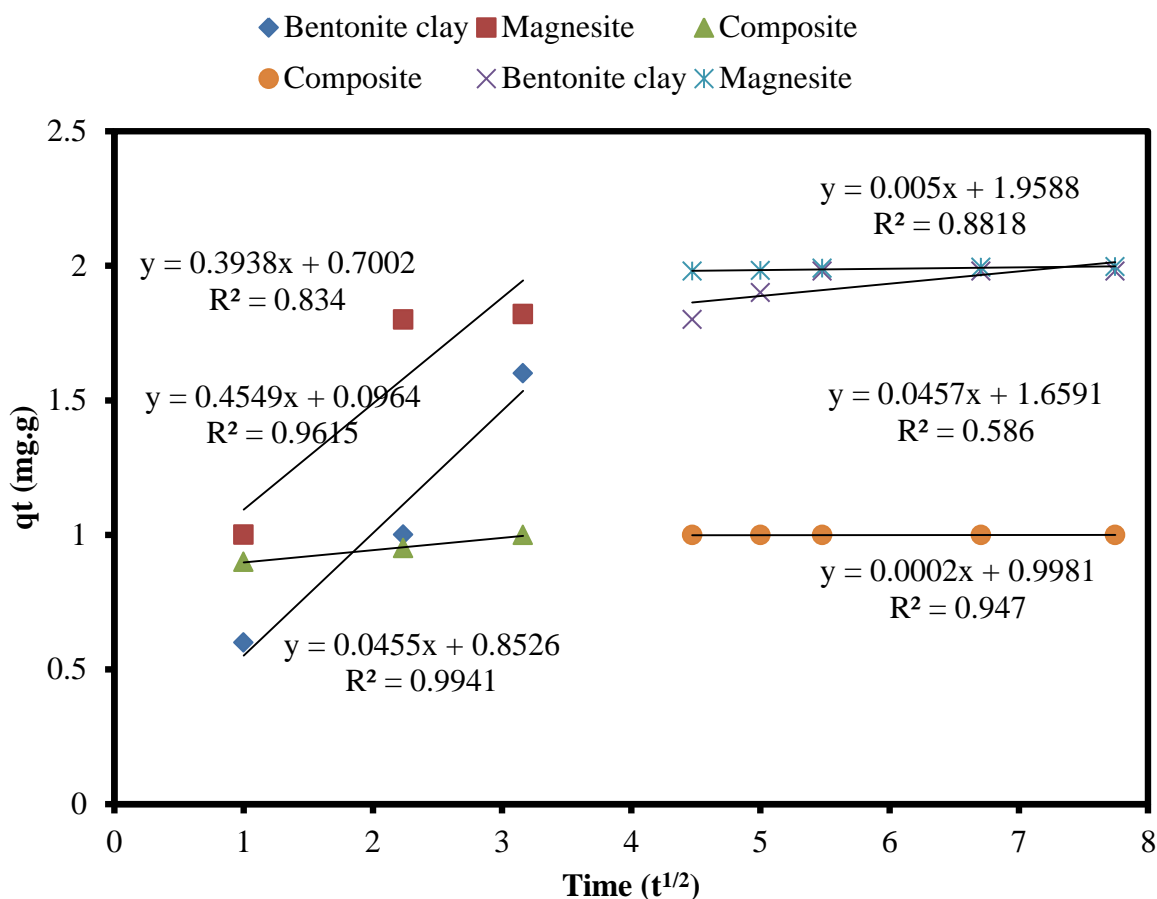


**Figure 4.10:** Intra-particle diffusion model for the adsorption of CR from aqueous solution using bentonite clay, pre-treated magnesite, and their nanocomposite.

#### 4.4 Adsorption isotherms

##### 4.4.1 Langmuir and Freundlich adsorption isotherm

Langmuir adsorption for the adsorption of CR dye onto bentonite clay, pre-treated magnesite, and their nanocomposite is shown in **Figure 4.11**.

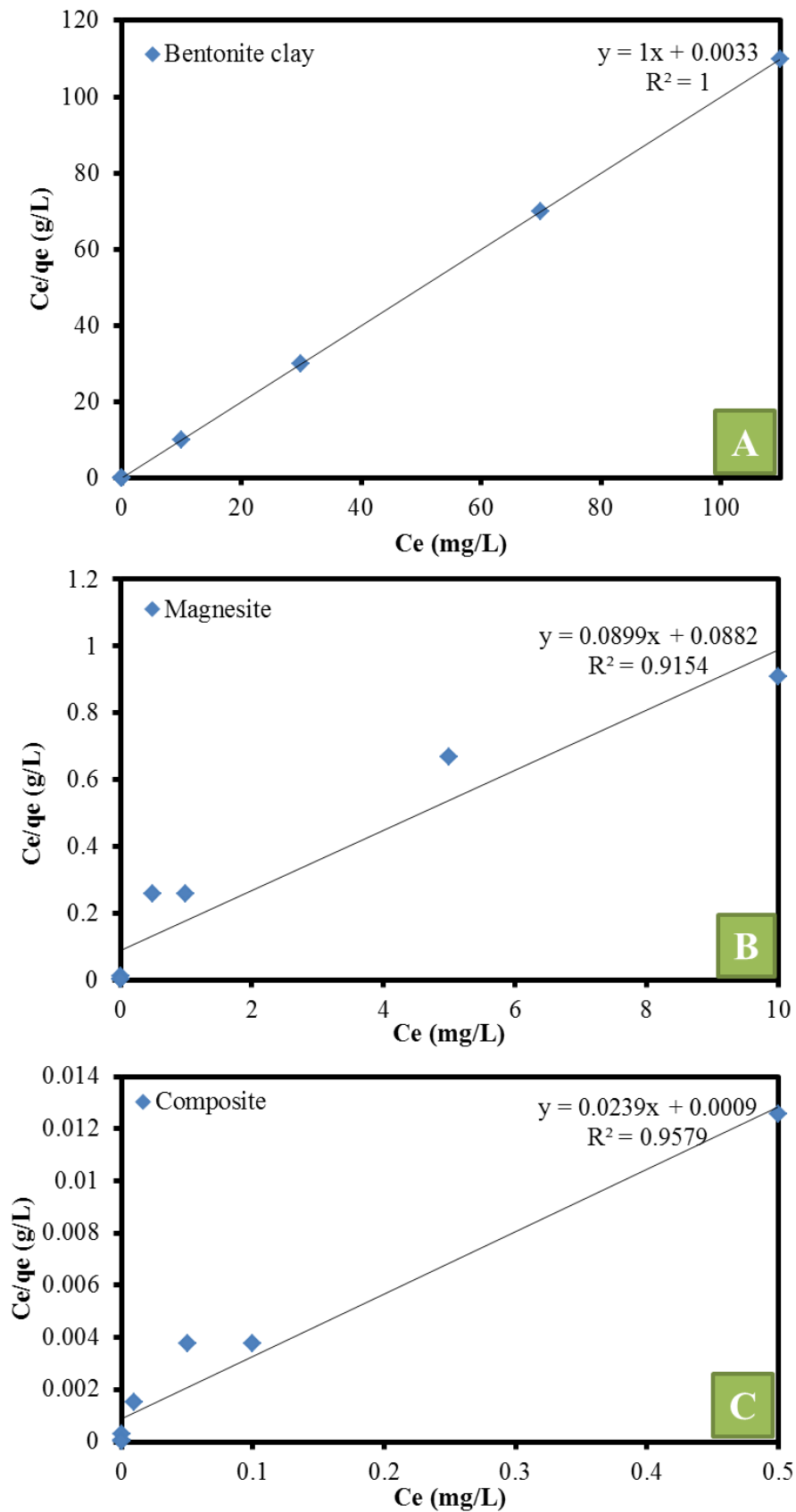


**Figure 4.11:** Langmuir adsorption isotherms for the adsorption of CR from aqueous solution using bentonite clay, pre-treated magnesite, and their nanocomposite.

Freundlich adsorption isotherm for the adsorption of CR dye onto bentonite clay, pre-treated magnesite, and their nanocomposite is shown in **Figure 4.12**.

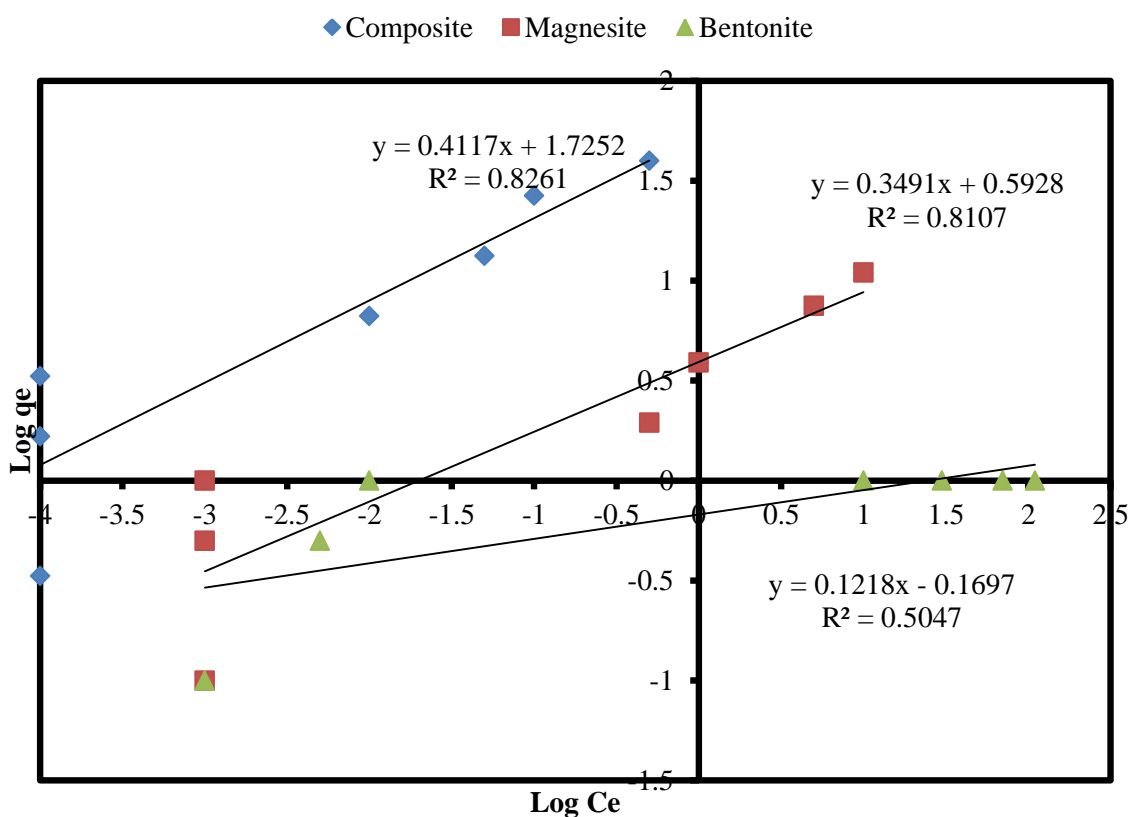


**Figure 4.12:** Freundlich adsorption for the adsorption of CR by bentonite clay, pre-treated magnesite, and their nanocomposite

Langmuir and Freundlich adsorption isotherm parameters for the adsorption of CR onto bentonite clay, pre-treated magnesite, and their nanocomposite are shown in **Table 4.3**.

**Table 4.3:** Langmuir and Freundlich adsorption isotherm parameters for the adsorption of CR onto bentonite clay, pre-treated magnesite, and their nanocomposite

Langmuir adsorption isotherm				
Materials	$q_m$	$b$ (L/mg)	$R_L$	$R^2$
Bentonite clay	1	303	$2.8 \times 10^{-5}$	1
Magnesite	11.1	1.02	$8.1 \times 10^{-3}$	0.92
Composite	41.8	26.6	$3.1 \times 10^{-4}$	0.96
Freundlich adsorption isotherm				
Material	$K_F$ (mg/g)	$n$	$R^2$	
Bentonite clay	1.48	8.2	0.50	
Magnesite	3.92	2.86	0.81	
Composite	53.1	2.43	0.83	

As shown in Table 3, the adsorption isotherms indicated that the removal of CR dye by bentonite clay, pre-treated magnesite, and their nanocomposite fitted well to Langmuir adsorption isotherm than the Freundlich adsorption isotherm hence indicating mono-layer adsorption. This was further proved by  $R_L$  value which is  $< 1$ , hence indicating that the reaction is favourable. The  $n$  value which is  $> 1$  for Freundlich adsorption isotherm further proved that the reaction is not favourable (Tran et al., 2017).

#### 4.4.2 Thermodynamics

Thermodynamics for the adsorption of CR dye onto bentonite clay, pre-treated magnesite, and their nanocomposite is shown in **Figure 4.13**.

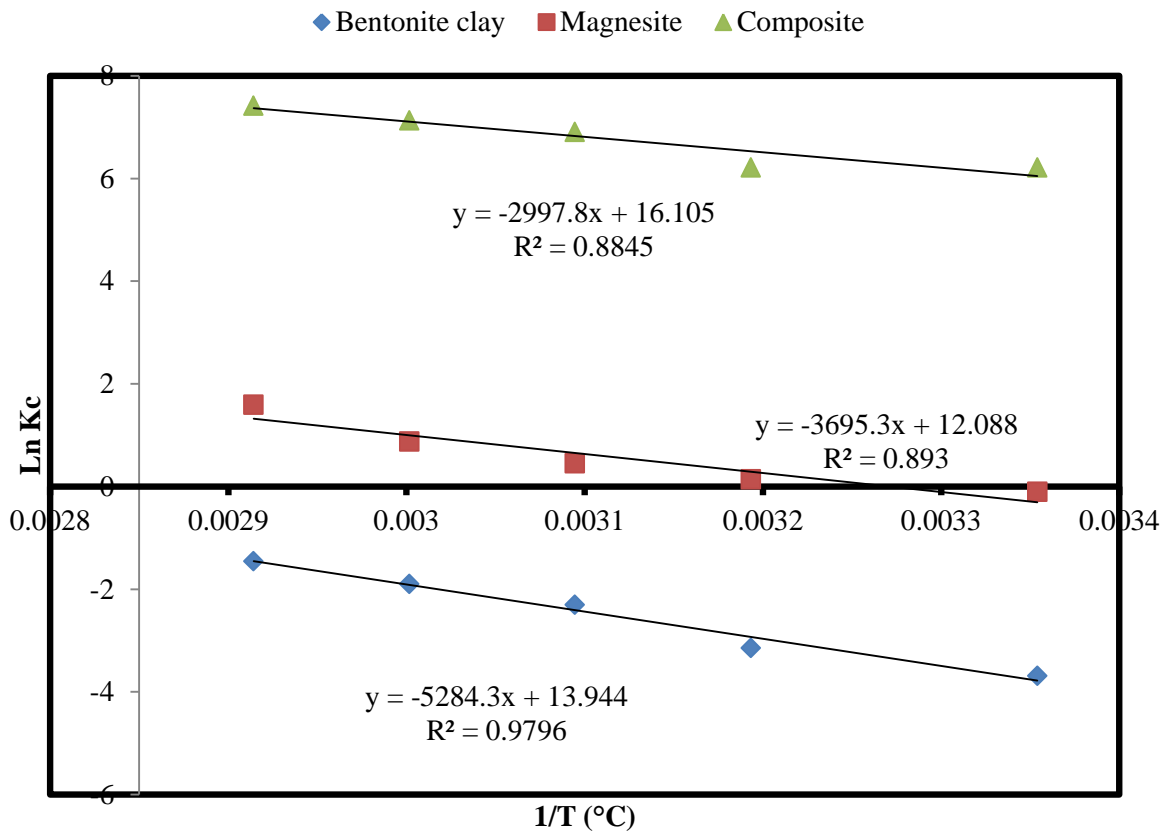


**Figure 4.13:** Thermodynamics for the adsorption of CR ions by bentonite clay, pre-treated magnesite, and their nanocomposite.

Thermodynamics for the adsorption of CR ions by bentonite clay, pre-treated magnesite, and their nanocomposite are shown in **Table 4.4**.

**Table 4.4:** Thermodynamics for the adsorption of CR onto bentonite clay, pre-treated magnesite, and their nanocomposite

	Thermodynamic studies			
Bentonite clay	$\Delta G^0$ (kJ mol <sup>-1</sup> )	$\Delta S^0$ (kJ mol <sup>-1</sup> K <sup>-1</sup> )	$\Delta H^0$ (kJ mol <sup>-1</sup> )	R <sup>2</sup>
298.15	9.144065	0.1	43.86	0.98
313.15	8.200812			
323.15	6.186284			
333.15	5.25466			
343.15	4.15186			
Magnesite	$\Delta G^0$ (kJ mol <sup>-1</sup> )	$\Delta S^0$ (kJ mol <sup>-1</sup> K <sup>-1</sup> )	$\Delta H^0$ (kJ mol <sup>-1</sup> )	R <sup>2</sup>
298.15	0.26117	0.1	30.67	0.89
313.15	-0.36387			
323.15	-1.20618			
333.15	-2.42488			
343.15	-4.53401			
Nanocomposite	$\Delta G^0$ (kJ mol <sup>-1</sup> )	$\Delta S^0$ (kJ mol <sup>-1</sup> K <sup>-1</sup> )	$\Delta H^0$ (kJ mol <sup>-1</sup> )	R <sup>2</sup>
298.15	-15.4044	0.13	24.88	0.89
313.15	-16.1794			
323.15	-18.5586			
333.15	-19.751			
343.15	-21.1647			

As shown in **Table 4.4**, the values of  $\Delta H^0$  (kJ mol<sup>-1</sup>) were observed to be 43.86, 30.67, and 24.88 for bentonite clay, pre-treated magnesite, and their nanocomposite respectively. This indicates that the reaction is endothermic. The positive  $\Delta S^0$  (kJ mol<sup>-1</sup> K<sup>-1</sup>) values confirms that the increase in the degree of randomness at solid/solution interface during the removal of CR ions from aqueous solution. The negative values of  $\Delta G^0$  (kJ mol<sup>-1</sup>) for the nanocomposite suggest the spontaneity and feasibility of CR adsorption whereas the positive  $\Delta G^0$  (kJ mol<sup>-1</sup>) for bentonite suggest a non-spontaneous nature of adsorption. Magnesite had negative values at temperature > 40 °C hence depicting a spontaneous reaction and at 25 °C it was non-spontaneous in nature.

#### 4.5 Treatment of authentic dye effluence

The efficiency of the synthesized nanocomposite for the removal of CR from synthetic and printing industry is shown in **Figure 4.14**.

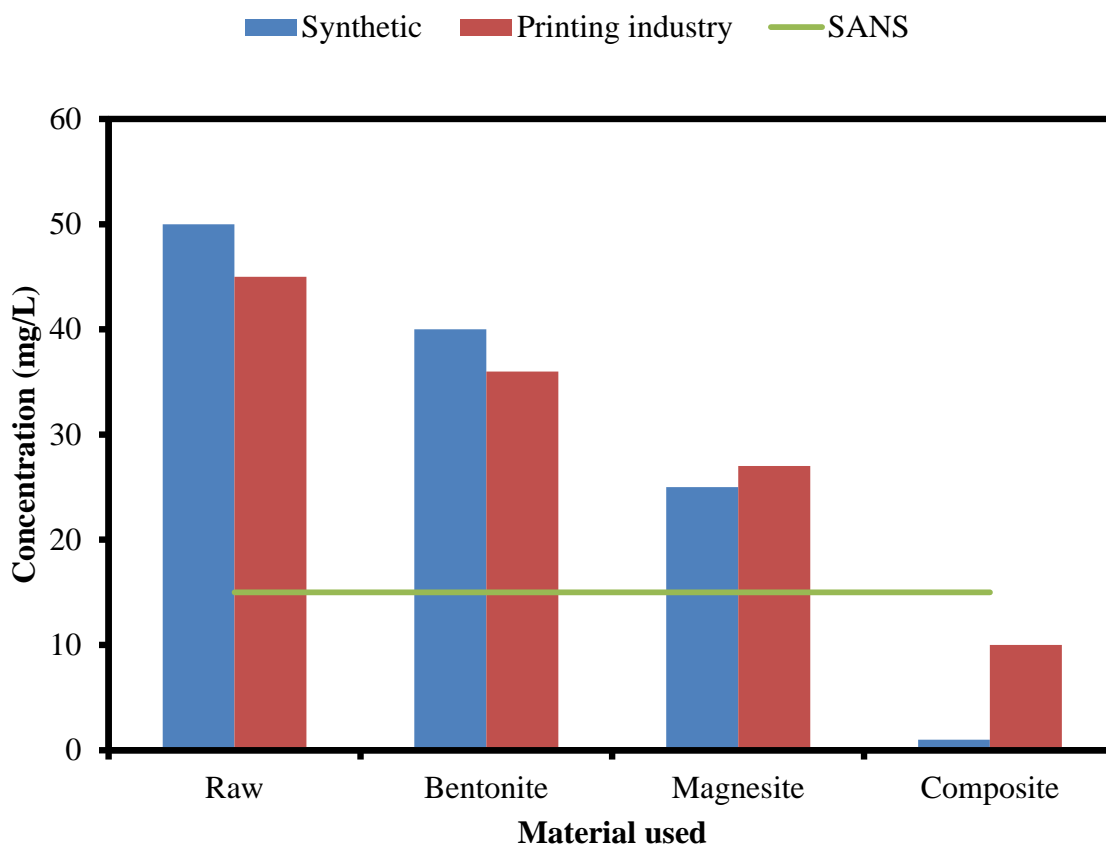


**Figure 4.14:** Efficiency of the synthesized nanocomposite for the removal of CR from synthetic and printing industry

As shown in **Figure 4.14**, the efficiency of the nanocomposite under optimised conditions was evaluated. Feed water from a synthetic solution and effluents from printing industry were observed to contain 50 and 45 mg/L respectively. After contacting bentonite clay, the level of CR was observed to have decreased but it was above the SANS 241 specification. After contacting the magnesite, the levels of CR in synthetic and authentic effluents were observed to have further decreased. Furthermore, the synthesized composite was observed to be effective for the treatment of synthetic dyes and effluents emanating from a printing industry. The composite managed to bring the effluent below SANS 241 specification, thus proving that the material can work on both synthetic and original samples.

#### 4.6 Desorption and regeneration studies

Desorption and regeneration gives useful insights about the possibility of the regeneration of adsorbent. To identify the suitable agent that can be used for desorption of CR adsorbed onto bentonite clay, pre-treated magnesite, and their nanocomposite, five solvents were used to desorb CR adsorbed onto bentonite clay, pre-treated magnesite, and their nanocomposite are shown in **Figure 4.15**.

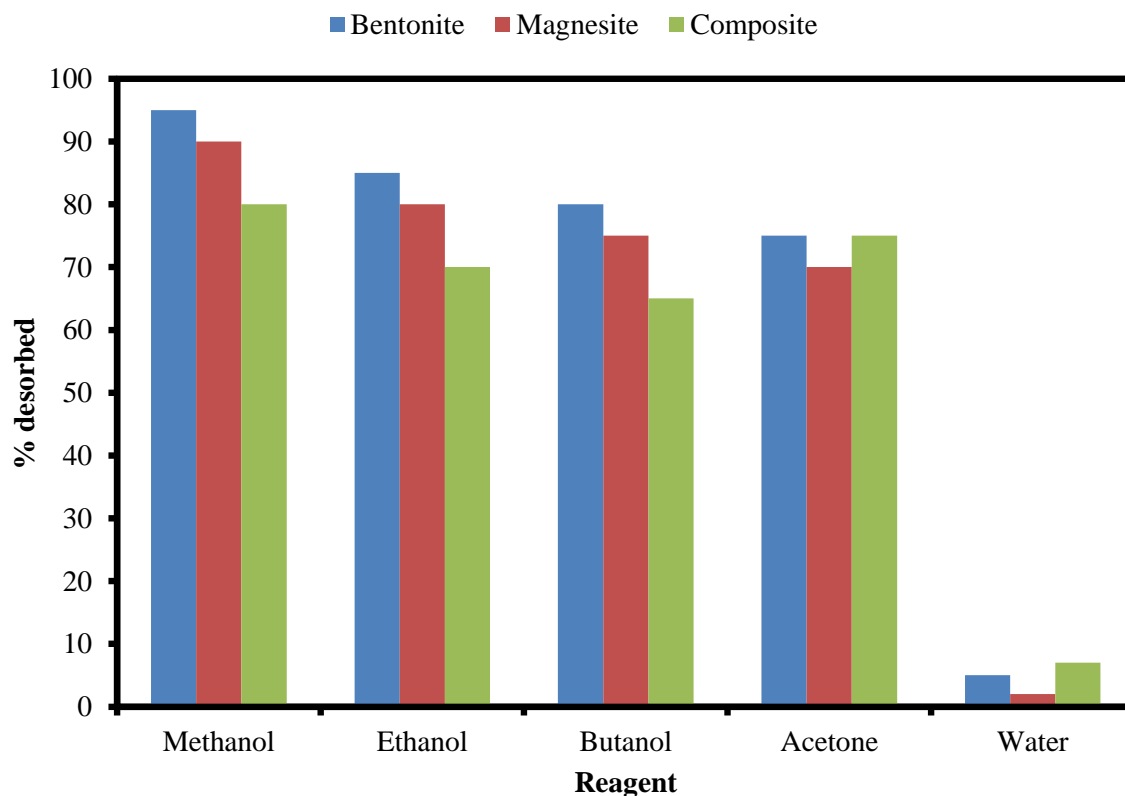


**Figure 4.15:** Desorption of CR from bentonite clay, pre-treated magnesite, and their nanocomposite using five different desorption agents.

As shown in **Figure 4.15**, different agents were used to remove CR from the matrices of bentonite clay, pre-treated magnesite, and their nanocomposite. The reactions indicated that methanol, ethanol, butanol, acetone and water depicted the best performance. Water was the worst of them all, hence indicating that water cannot be used to remove CR dye from the matrices of the bentonite clay, pre-treated magnesite, and their nanocomposite. Methanol presents the highest desorption efficiency hence it will be used for a subsequent study. Desorption cycles of CR using methanol were examined and the results are shown in **Figure 4.16**.

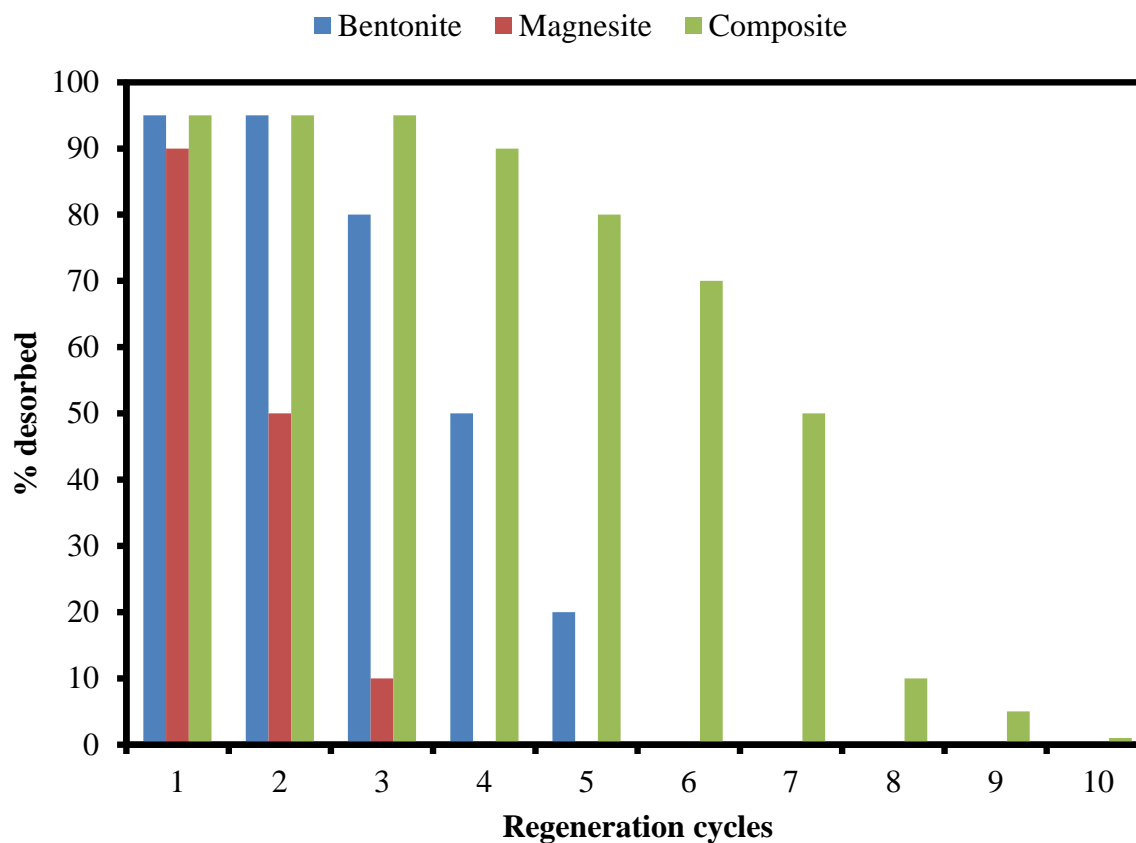


**Figure 4.16:** Desorption cycles of CR from bentonite clay, pre-treated magnesite, and their nanocomposite matrices using methanol.

As shown in **Figure 4.16**, bentonite clay showed stability in the first two circles, thereafter, the efficacy was compromised. This may be attributed to the loss of exchangeable cations during regeneration. Magnesite showed poor regeneration ability. This is due to solubility of magnesium from the feed matrices. The nanocomposite demonstrated superior ability in relation to individual materials. This may be attributed to preparation technique that enhanced its mechanical strength.

#### 4.7 Comparison of the synthesized nanocomposite with other adsorbents

The comparison of the efficiency of bentonite clay, pre-treated magnesite, and their nanocomposite with other adsorbents used for CR removal is shown in **Table 4.5**.

**Table 4.5:** Comparison of the efficiency of bentonite clay, pre-treated magnesite, and their nanocomposite with other adsorbents used for CR removal

Material	Adsorption capacity	Reference
Bentonite clay	1 mg/g	This work
Pre-treated magnesite	11 mg/g	This work
Magnesite/bentonite composite	39 mg/g	This work
Mg–Al–LDH	37 mg/g	(Xu et al., 2018)
Natural serpentine	93.4 mg/g	(Shaban et al., 2018)
Waste banana pith	20 mg/g	(Namasivayam and Kanchana, 1992)
Biogas waste slurry	9.5 mg/g	(Namasivayam and Yamuna, 1992)
Waste red mud	4.05 mg/g	(Namasivayam and Arasi, 1997)
Activated bentonite	7 mg/g	(Toor et al., 2015)
Waste orange peel	22.4 mg/g	(Namasivayam et al., 1996)
Australian kaolins	5.4 mg/g	(Vimonses et al., 2009)

As shown in **Table 4.5**, the adsorption capacity of bentonite clay, pre-treated magnesite, and their nanocomposite is better than most of the adsorbents in literature. The other materials have low adsorption capacity except Natural serpentine. However, this may be attributed to other factors such as residence time during adsorption and material modification. Synergies of the adsorption materials also play a significant role in the removal of pollutants from an aqueous system. This indicates that this material has comparative ability and it can be deployed for the removal of CR from printing and other industries.

#### 4.8 Mechanisms of Congo Red (CR) removal

The mechanism of CR adsorption onto bentonite clay, pre-treated magnesite, and their nanocomposite involves the inter-actions of different facets of the CR molecule with bentonite clay, pre-treated magnesite, and their nanocomposite. When CR, a typical anionic dye, is dissolved in water, the two  $-SO_3$ -groups give the CR molecule negative charge. On the other hand, bentonite clay, pre-treated magnesite, and their nanocomposite, have a positive net surface charge. The protonated hydroxyl groups (i.e.,  $-OH^{2+}$ ) on the surface of the nanocomposite attract the negatively charged  $-SO_3$ -groups, and this electrostatic interaction is supposed to be part of the mechanisms of CR adsorption. Furthermore, electrostatic attraction plays a key role in the adsorption of anionic dyes such as CR onto positively

charged adsorbent because the composite contains  $Mg^{2+}$  that can form a complex with the  $-SO_3$  group. Ion exchange high valent species from bentonite clay, pre-treated magnesite, and their nanocomposite matrices and interlayers also contribute to the removal of CR. Adsorption to surface charges of bentonite clay, pre-treated magnesite, and their nanocomposite also governs the removal of CR from an aqueous system.

## CHAPTER FIVE

### CONCLUSIONS AND RECOMMENDATIONS

#### 5.1 Conclusions

From the findings of this study, it can be concluded that this study achieved the outlined objectives and successfully proved the developed hypothesis. The nanocomposite was successfully synthesized using mechanochemically synthesis technique and effectively tested for the removal of CR from aqueous solution. Experimental results revealed that optimum conditions that are suitable for the treatment of CR dye are 20 minutes, 0.5 g of dosage, 120 mg/L, 250 rpm, and pH = 7. Greater than 99% removal efficacy of CR were achieved for the composite and it was thus below the South African National Standard (SANS) 241 specifications. The composite showed superior performance in relation to individual materials. Methanol was used as a desorpting agent and the efficacy was observed to be 1, 0, and 2 regeneration cycles for bentonite, pre-treated magnesite and their composite respectively. Adsorption kinetic studies revealed that bentonite clay, pre-treated magnesite, and their nanocomposite fitted very well to pseudo-second-order kinetics than pseudo-first-order kinetics. The regression analysis was observed to be 1, 0.9, and 0.9 for bentonite clay, pre-treated magnesite, and their nanocomposite respectively. Adsorption isotherms indicated that CR removal by bentonite clay, pre-treated magnesite, and their nanocomposite fitted well to Langmuir adsorption isotherm than the Freundlich adsorption isotherm hence indicating mono-layer adsorption. This was further proved by  $R_L$  value which is  $< 1$ , hence indicating that the reaction is favourable. The  $n$  value which is  $> 1$  for Freundlich adsorption isotherm further proved that the reaction is not favourable. Thermodynamic values for CR removal were observed to be:  $\Delta H^0$  (kJ mol<sup>-1</sup>) = 43.86, 30.67, and 24.88 for bentonite clay, pre-treated magnesite, and their nanocomposite respectively. This indicates that the reaction is endothermic. The positive  $\Delta S^0$  (kJ mol<sup>-1</sup> K<sup>-1</sup>) values for bentonite clay and 25 °C for pre-treated magnesite confirms that there is an increase in the degree of randomness at solid/solution interface during the removal of CR ions from aqueous solution. The negative values of  $\Delta G^0$  (kJ mol<sup>-1</sup>) for 40 – 70 on bentonite and the entire range for the nanocomposite suggest the spontaneity and feasibility of CR adsorption whereas the positive  $\Delta G^0$  (kJ mol<sup>-1</sup>) for bentonite suggest a non-spontaneous nature of adsorption. As such, magnesite/bentonite clay nanocomposite demonstrated superior adsorption capacity in relation to individual

materials and other materials reported in literature. From this comparative study, it was proven that the synthesized nanocomposite can be successfully used for the removal of CR from aqueous solution. This material can be used for the treatment of dyes from the printing industries.

## 5.2 Recommendations

The primary aims from this study were adequately achieved; however, there are research gaps that will need to be investigated in future research. As such, it can be recommended that:

- Column studies are conducted to evaluate the ability of the developed materials for the removal of CR on a continuous mode.
- Techno-economic evaluation of the proposed material be evaluated to check the initial costs of the technology
- Doping of the material to increase the adsorption capacity, hence increasing the adsorption efficiency of the proposed materials.
- Life cycle assessment of the proposed system, this will be an indicator of how environmentally friendly is the proposed technology.

## REFERENCES

- Abdel-Khalek, M. A., Abdel Rahman, M. K. & Francis, A. A. 2017. Exploring the adsorption behavior of cationic and anionic dyes on industrial waste shells of egg. *Journal of Environmental Chemical Engineering*, 5, 319-327.
- Adensola, B., Ogundipe, K., Sangosanya, K. T. & Akintola, B. D., 2016. Comparative study on the biosorption of Pb(II), Cd(II) and Zn(II) using lemon grass (*Cymbopogon citratus*): kinetics, isotherms and thermodynamics. *Journal of Chemistry Interface*. 2, 89-102.
- Alver, E., Bulut, M., Metin, A. Ü. & Çiftçi, H. 2017. One step effective removal of Congo Red in chitosan nanoparticles by encapsulation. *Spectrochimica Acta Part A: Molecular and Biomolecular Spectroscopy*, 171, 132-138.
- Atwood, J. L., Gokel, G. W., Barbour, L. J. 2017. *Comprehensive Supramolecular Chemistry II, Volume 1, Second Edition*, Elsevier
- Ausavasukhi, A., Kamposoen, C. & Kengnok, O. 2016. Adsorption characteristics of Congo red on carbonized leonardite. *Journal of Cleaner Production*, 134, 506-514.
- Banat, I. M., Nigan, P., Singh, D. & Marchant, R. 1996. Microbial decolorization of textile - dye-containing effluents. A review of *Bioresources Technology Journal*, 58 (3), 217 - 227.
- Belhachemi, M., Belalaa, Z., Lahcenea, D. & Addounb, F. 2009. Adsorption of phenol and dye from aqueous solution using chemically modified date pits activated carbons. *Desalination and Water Treatment*, 7, 182-190.
- Belhouchat, N., Zaghouane-Boudiaf, H. & Cesar, V., 2016. Removal of anionic and cationic dyes from aqueous solution with activated organo-bentonite/ sodium alginate encapsulated beads. *Journal of Applied Clay Science* 135, 9-5.
- Benkli, Y. E., Mittal, A. L. & Broadbent, A. D., 2005. Modification of organo- zeolites surface for the removal of reactive azo dye in fixed- bed reactors. *Water Research Journal*, 39, 487- 493.

- Bhatnagar, A. & Jain, A. K., 2005. A comparative adsorption study with different industrial wastes adsorbents for the removal of cationic dyes from water. *Journal of Colloid Interface Sci*, 49-55.
- Bhatnagar, A., Kumar, E., Sillanpaa, M., 2011. Fluoride removal from water by adsorption: a review. *Chemical Engineering Journal*.
- Birchal, V. S. S., Rocha, S. D. F. & Ciminelli, V. S. T. 2000. Effect of magnesite calcination conditions on magnesia hydration. *Minerals Engineering*, 13, 1629-1633.
- Broadbent 2001. *Basic principles of textile coloration*. Society of Dyers and Colourists, West Yorkshive, England.
- Brown, D., 1987. Effects of colorants in the aquatic environmental Ecotoxicol. *Environmental Safety* 13, 139-147.
- Burkinshaw, S., 2016. *Physico-chemical aspects of textile coloration*. Wiley, Hoboken, New Jersey.
- Cadena, F., Rizvi, R., Peters, R.W., 1990. Feasibility studies for the removal of heavy metals from solution using tailored bentonite, in: *Hazardous and Industrial Wastes Twenty-second Mid-Atlantic Industrial Waste Conference*, Drexel University.
- Carmen, Z. & Daniela, S., 2012. Textile organic dyes- characteristics, polluting effects and separation/ elimination procedures from industrial effluents- a critical overview. Croatia, In Tech Press, 55 - 86.
- Carnejo, J., Celis, R., Pavlovic, I. & Ulibarri, M. A., 2008. Interactions of pesticides with clays and layered double hydroxydes: a review. *Clay Minerals*, 43, 55-175.
- Casselmann, K., L 1980. *Craft of the Dyer: Colour from plants and Lichens of the Northeast Toronto* Toronto: University of Toronto Press.
- Chahkandi, M. 2017. Mechanism of Congo red adsorption on new sol-gel-derived hydroxyapatite nano-particle. *Materials Chemistry and Physics*, 202, 340-351.
- Charlie, S., Ratto, M. & Rovatti, M., 2000. Mercury removal from water by ion exchange resins adsorption. *Water Research Journal*, 34, 2971- 2978.

- Chatterjee, S., Lee, D. S. & Lee, M. W., 2009. Congo red adsorption from aqueous solutions by using chitosan hydrogel beads impregnated with nonionic or anionic surfactants. *Bioresource Technology*. 100, 3862-3868.
- Chawla, S., Uppal, H., Yadav, M., Bahadur, N. & Singh, N. 2017. Zinc peroxide nanomaterial as an adsorbent for removal of Congo red dye from waste water. *Ecotoxicology and Environmental Safety*, 135, 68-74.
- Chen, Chen, Luan & Zhinguo 2016. Characterization of anion- cationic surfactants modified montmorillonite and its application for the removal of methyl orange. *Journal of Chemical Engineering* 171 (3), 1150- 1158.
- Chen, H., Zhao, J., Zhong, A. & Jin, Y. 2011. Removal capacity and adsorption mechanism of heat-treated palygorskite clay for methylene blue. *Chemical Engineering Journal*, 174, 143-150.
- Cheremisinoff, N. & Moressi, A., 1978. Carbon adsorption applications, in Cheremisinoff NP and Ellerbusch (EDS.). In: *Carbon Adsorption Handbook*. Ann Arbor: Ann Arbor Science, 1- 53.
- Crini, G., 2006. Non- conventional low- cost adsorbents for dye removal: a review. *Bioresources Technology*. 97, 1061- 1085.
- Crini, G. and Badot. P.M, 2008. Application of chitosan, a natural aminopolysaccharide, for dye removal from aqueous solutions by adsorption processes using batch studies: a review of recent literature. *Journal of Progress Polymaterial Science*. 33, 399-447.
- Cripps, C; Bumpus, J; Dust, S, 1990. *Applied Environmental Microbiology*, 56, 1114-1118.
- Dawwod & Sen 2014. Review on dye removal from its aqueous solutions into alternative cost effective and non- conventional adsorbents. *Journal of Chemical Process Engineering*. 1, 104.
- De León, M. A., Sergio, M. & Bussi, J. 2013. Iron-pillared clays as catalysts for dye removal by the heterogeneous photo-Fenton technique. *Reaction Kinetics, Mechanisms and Catalysis*, 110, 101-117.

- Dhal, J. P., Sethi, M., Mishra, B. G. & Hota, G. 2015. MgO nanomaterials with different morphologies and their sorption capacity for removal of toxic dyes. *Materials Letters*, 141, 267-271.
- Dogan, Mustafa, Akgul, Eda, Sema & Aysegil 2007. Adsorption equilibrium and kinetic of reactive black 5 and reactive red 239 in aqueous solution onto surfactant- modified zeolites. *Journal of Chemical Engineering Data*, 52: 1615-1620.
- Dotto, G. L., Lima, E. C. & Pinto, L. a. A. 2012. Biosorption of food dyes onto *Spirulina platensis* nanoparticles: Equilibrium isotherm and thermodynamic analysis. *Bioresource Technology*, 103, 123-130.
- Dukic, A. B., Kumric, K. R., Vukelic, M. S. & Kurko, L. L., 2015. Simultaneous removal of Pb, Cu, Zn and Cd from highly acidic solutions using mechanochemically synthesized montmorillonite-kaolinite/TiO<sub>2</sub>. *Applied Clay Science*, 103, 20-27.
- DWAF, 2002. National water management strategies, South Africa: Proposed 1st ed. Department of water affairs and forestry.
- Elass, K., Laachach, A., Alaoui, A., Azzi. M., 2011. Removal of methyl violet from aqueous solution using a stevensite-rich clay from Morocco. *Applied Clay Science*. 54, 90–96.
- Farooqi, A., Masuda, H. & Firdous, N., 2007. Toxic fluoride and Possible contaminant sources and arsenic contaminated groundwater in the Lahore and Kasur districts, Punjab, Pakistan. *Environmental Pollution Journal* 145, 839- 849.
- Febrianto, J., 2009. Equilibrium and kinetic studies in adsorption of heavy metals using biosorbent: A summary of recent studies. *Journal of Hazardous Materials*, Volume 162, 616 - 645.
- Forgacs, E., Cserhati, T. & Oras, G. 2004. Removal of synthetic dyes from wastewater: a review *Environ International*. 30, 953-971.
- Freundlich, H. 1906. Over the adsorption in solution. *Zeitschrift fur Physikalische Chemie*, 57, 385-470.
- FRTR, 2012. Remediation technologies screening matrix and references guide version 4.0 - remediation technology. Washington, DC, Federal Remediation Technologies Roundtable.

- Gao, B.-Y., Yue, Q.-Y., Wang, Y. & Zhou, W.-Z. 2007. Color removal from dye-containing wastewater by magnesium chloride. *Journal of Environmental Management*, 82, 167-172.
- George, E., 1998. Physical and Chemical properties of some bentonite deposits of kimolos island. *The Journal of Applied Clay Science*, 79- 98.
- Ghaemi, N., Madaeni, S. S., Daraei, P., Rajabi, H., Shojaeimehr, T., Rahimpour, F. & Shirvani, B. 2015. PES mixed matrix nanofiltration membrane embedded with polymer wrapped MWCNT: Fabrication and performance optimization in dye removal by RSM. *Journal of Hazardous Materials*, 298, 111-121.
- Gitari, M. W., Petrik, L. F. & Etchebers, O., 2006. Treatment of acid mine drainage with fly ash. *The Journal of Environmental Science and Health. Part A: Toxic/ Hazardous Substances and Environmental Engineering*, 1729 - 1747.
- Gitari, M. W., Petrik, L. F. & Key, D. L., 2008. Passive neutralisation of acid mine drainage by fly ash and its derivatives: A column leaching study. *The Journal of Fuels*, 1637 - 1680.
- Gosavi, V. & Shama, S., 2013; 3. A general review on various treatment methods for textile wastewater. *Journal of Environmental Science Composite Science of Engineering Technology*, 29- 39.
- Gu, C., Jia, H., Li, H., Teppen, B. J., Boyd, S. A., 2010. Synthesis of highly reactive subnano-sized zero- valent iron using smectite clay templates. *Environmental Science Technology* 44, 4258- 4263.
- Gupta, N., Kushwaha, A. & Chattopadhyaya, M., 2012. Adsorption studies of cationic dyes onto Ashoka (*Saraca asoca*) kaf powder. *Journal of Taiwan Institute Chemical Engineering*, 43: 604.
- Gupta, S. K., 2016. Synthesis and performance evaluation of a new polymeric composite for the treatment of textile wastewater. *Journal of Indian Engineering of chemical resources*, 55, 13 - 20.

- Hai, Y., Li, X., Wu, H., Zhao, S., Deligeer, W., Asuha, S., 2015. Modification of acid-activated kaolinite with TiO<sub>2</sub> and its use for the removal of azo dyes. *Applied Clay Science*. 114, 558–567.
- Han, Z. X.; Zhu, Z.; Wu, D. D.; Wu, J.; Liu, Y. R., 2014. Adsorption kinetics and thermodynamics of acid blue 25 and methylene blue and methylene blue dye solutions on natural sepiolite. *Journal of Synthetic Reaction Inorganic Matters*. 44, 140-147.
- Hao, O., Kim, H. & Chiang, P., 2000. Decolorization of wastewater. *Critical Review of Environmental Science Technology* 30, 449- 505.
- Hossain, I., 2014. Investigation into cotton knit dyeing with reactive dyes to achieve right first time (RFT) shade. Master Thesis. Daffodil International University. Bangladesh.
- Ho, Y. S., Chiu, W. T. & Wang, C. C. 2005. Regression analysis for the sorption isotherms of basic dyes on sugarcane dust. *Bioresource Technology*, 96, 1285-1291.
- Ho, Y. S. & McKay, G. 1999. Pseudo-second order model for sorption processes. *Process Biochemistry*, 34, 451-465.
- Ho, Y. S., Ng, J. C. Y. & McKay, G. 2000. Kinetics of pollutant sorption by biosorbents: Review. *Separation and Purification Methods*, 29, 189-232.
- Hou, R., Gao, Y., Zhu, H., Yang, G., Liu, W., Huo, Y., Xie, Z. & Li, H. 2017. Coupling system of Ag/BiOBr photocatalysis and direct contact membrane distillation for complete purification of N-containing dye wastewater. *Chemical Engineering Journal*, 317, 386-393.
- Hu, K. H., Zhao, D. F. & Liu, J. S. 2012. Synthesis of nano-MoS<sub>2</sub>/bentonite composite and its application for removal of organic dye. *Transactions of Nonferrous Metals Society of China (English Edition)*, 22, 2484-2490.
- Hu, M., Yan, X., Hu, X., Zhang, J., Feng, R. & Zhou, M. 2018. Ultra-high adsorption capacity of MgO/SiO<sub>2</sub> composites with rough surfaces for Congo red removal from water. *Journal of Colloid and Interface Science*, 510, 111-117.
- Hu, Z., Chen, H., Ji, F. & Yuan, S. 2010. Removal of Congo Red from aqueous solution by cattail root. *Journal of Hazardous materials*, 173, 292-297.

- IARC, 2010. Monographs on the evaluation of carcinogenic risks to humans vol 99 some aromatic amines, organic dyes, and related exposures. Lyon, France.
- Igbal, M., 2008. Textile dyes, Pakistan: Rahber Publishers.
- Igbal, M., Ahmad, I. & Bhatti, I. A., 2014. Re-utilization option of industrial wastewater treated by advanced oxidation process. Pak. Journal of Agricultural Science 51(4), 1041-1047.
- Jivasvipongpun, K., Nasanit, R., Niruntasook, J. & Chotikasatian, B., 2007. International Journal Science Technology, 12, 6-11.
- Johnson, R., 2005. Drinking Water Treatment Methods. [Online] Available at: <http://www.cyber-nook.com/water/solutions.html>
- Kanade, S., Shinde, D. R. & Kanade, K. G. 2017. Heterostructured ti-doped ZnO/Ag metal: An efficient photocatalyst for dye degradation in sunlight. Desalination and Water Treatment, 71, 388-398.
- Kant, R., 2012. Adsorption of dye eosin from an aqueous solution on two different samples of activated carbon by static batc method. Journal of Water Resources Protection. 4, 93-98.
- Karthikeyan, S., Boopathy, R. & Sekaran, G. 2015. In situ generation of hydroxyl radical by cobalt oxide supported porous carbon enhance removal of refractory organics in tannery dyeing wastewater. Journal of Colloid and Interface Science, 448, 163-174.
- Kataria, N. & Garg, V. K. 2017. Removal of Congo red and Brilliant green dyes from aqueous solution using flower shaped ZnO nanoparticles. Journal of Environmental Chemical Engineering, 5, 5420-5428.
- Khan, T., Khan, E. & Shahjahan, 2015. Removal of basic dyes from aqueous solution by adsorption onto binary iron-manganese oxide coated kaolinite: non-linear isotherm and kinetics modelling. Journal of Applied Clay Science. 107, 70-77.
- Khenifi, A., Bouberka, K., Kameche, F. & Derriche, Z. 2007. Adsorption a study of an industrial dye by an organic clay. Adsorption, 13, 149 - 158.

- Khenifi, A., Zohra, B. & Kahina, B., 2009. Removal of 2, 4- DCP from wastewater by CTAB/ bentonite using one- step and two- step methods. *The Chemical Engineering Journal*, 345- 354.
- Kirk-O, 1994. *Encyclopedia Chemical Technology*. Edition 8, 542-672.
- Kumar, P., Teng, T. T., Chand, S. & Wasewar, K. L. 2011. Fenton oxidation of carpet dyeing wastewater for removal of COD and color. *Desalination and Water Treatment*, 28, 260-264.
- Kurniawan, T., Chan, G., Lo, W. & Babel, S., 2006. Physico- chemical treatment techniques for wastewater laden with heavy metals. *Chemical Engineering Journal* 118, 83- 98.
- Lagergren, S. 1898. About the theory of so-called adsorption of soluble substances. *Handlingar*, 24, 1-39.
- Langmuir, I. 1916. The constitution and fundamental properties of solids and liquids. Part I. Solids. *The Journal of the American Chemical Society*, 38, 2221-2295.
- Langmuir, I., 1918. The adsorption of gases on plane surfaces of glass, mica and platinum. *Amplified Chemistry Society*, 1361- 4003.
- Letterman, R. D., 1999. *Water quality and treatment: a handbook of community water supplies*. American Water Works Association. New York: McGraw Hill Publications.
- Liles, J., N 1990. *The Art and Craft of Natural Dyeing: Traditional Recipes for Modern Use*. Knoxville, Tenn: University of Knoxville Press.
- Li, L., Li, X., Duan, H., Wang, X., Luo, C., 2014. Removal of Congo Red by magnetic mesoporous titanium dioxide-graphene oxide core-shell microspheres for water purification.. *Journal of Dalton Transition*. 43, 8431-8438.
- Li, Q., Yue, Q. Y., Sun, H. J., Su, Y., Gao, B. Y., 2010. A comparative study on the properties, echanisms and process designs for the adsorption of non-ionic dyes onto cationic-polymer/bentonite. *Journal of Environmental Management*. 91, 1601-1611.
- Lima, E. C. A., M.A. Machado, F.M. 2015. Kinetic and equilibrium models of adsorption. In: BERGMANN, C. P. M., F.M. (ed.) *Carbon nanomaterials as adsorbents for*

- environmental and biological applications. Switzerland: Springer International publishing, 33-69.
- Liu, R. L., Chiu, H. M. & Yeh, R. Y., 2002. Colloid interaction and coagulation of dye wastewater with extra application of magnetites. *Int. Journal of Environmental Studies*. 59, 143-158.
- Madej, D., 2017. Size-dependent hydration mechanism and kinetics for reactive MgO and Al<sub>2</sub>O<sub>3</sub> powders with respect to the calcia-free hydraulic binder systems designed for refractory castables. *Journal of Material Science*, 52 (12), 7578-7590.
- Mahmoud, M. E., Abdou, A. E. H., Shehata, A. K., Header, H. M. A. & Hamed, E. A. 2018. Sustainable super fast adsorptive removal of Congo red dye from water by a novel technique based on microwave-enforced sorption process. *Journal of Industrial and Engineering Chemistry*, 57, 28-36.
- Martinez - Hutile, A., C & Brillas, E. 2009. Decontaminants of wastewaters containing synthetic organic dyes by electrochemical methods: A general review. *Applied Cationic dyes: Environment*, 87, 105 - 145.
- Masindi, V. 2017. Recovery of drinking water and valuable minerals from acid mine drainage using an integration of magnesite, lime, soda ash, CO<sub>2</sub> and reverse osmosis treatment processes. *Journal of Environmental Chemical Engineering*, 5, 3136-3142.
- Masindi, V. & Gitari, M. W. 2016. Removal of boron from aqueous solution using cryptocrystalline magnesite. *Journal of Water Reuse and Desalination*.
- Masindi, V; Gitari, M. W; Tutu, H; and De Beer, M, 2014a. Application of magnesite-bentonite clay composite as an alternative technology for removal of arsenic from industrial effluents. *Journal of Toxicology Environmental Chemistry*. 96, 1435-1451.
- Masindi, V; Gitari, M.W; Tutu, H; De Beer, M, 2014b. Neutralization and attenuation of metal species in acid mine drainage and mine leachates using magnesite: a batch experimental approach, in: Sui, Sun, Wang(Eds.),. *An Interdisciplinary Response to Mine Water Challenges*, China Univ, 640-644.

- Masindi, V., Gitari, M. W., Tutu, H. & De Beer, M. 2015a. Passive remediation of acid mine drainage using cryptocrystalline magnesite: A batch experimental and geochemical modelling approach. *Water SA*, 41, 677-682.
- Masindi, V., Gitari, M. W., Tutu, H. & Debeer, M. 2017. Synthesis of cryptocrystalline magnesite–bentonite clay composite and its application for neutralization and attenuation of inorganic contaminants in acidic and metalliferous mine drainage. *Journal of Water Process Engineering*, 15, 2-17.
- Masindi, V. & Gitari, W. 2013. Adsorption of Oxyanions of As, B, Cr, Mo and Se from Coal Fly Ash Leachates Using  $Al^{3+}/Fe^{3+}$  Modified Benonite Clay, South Africa, University of Venda.
- Masindi, V., Gitari, W. M. & Ngulube, T. 2015b. Kinetics and equilibrium studies for removal of fluoride from underground water using cryptocrystalline magnesite. *Journal of Water Reuse and Desalination*, 5, 282-292.
- Messina, P. V. a. S. P. C., 2006. Adsorption of reactive dyes on titania-silica mesoporous materials. *Journal of Colloid Interface Science*. 299, 305-320.
- Miandad, R., Kumar, R., Barakat, M. A., Basheer, C., Aburizaiza, A. S., Nizami, A. S. & Rehan, M. 2018. Untapped conversion of plastic waste char into carbon-metal LDOs for the adsorption of Congo red. *Journal of Colloid and Interface Science*, 511, 402-410.
- Mishra, G. & Tripathy, M, 1993. A critical of the treatment for decolorization of textile effluents. *Colourage*. 40, 35-38.
- Mittal, A; Krishnan, L; Gupta, V.K, 2005a. Removal and recovery of Congo red from wastewater using an agricultural waste materials-de-oiled soya. *Separation and Purification Technology* 43, 125-133.
- Mittal, A., Krishnan, L. & Gupta, V., 2005b. Removal and recovery of malachite green from wastewater using agricultural waste material, de-oiled soya, sep. *Purification Technology*. 43, 125- 133.
- Mohy Eldin, M. S., Aly, K. M., Khan, Z. A., Mekey, A. E., Saleh, T. S. & Elbogamy, A. S. 2016a. Development of novel acid–base ions exchanger for basic dye removal:

- phosphoric acid doped pyrazole-g-polyglycidyl methacrylate. *Desalination and Water Treatment*, 57, 24047-24055.
- Mohy Eldin, M. S., Gouda, M. H., Abu-Saied, M. A., El-Shazly, Y. M. S. & Farag, H. A. 2016b. Development of grafted cotton fabrics ions exchanger for dye removal applications: methylene blue model. *Desalination and Water Treatment*, 57, 22049-22060.
- Mouloud, L., Jean-Philippe, B., Baodu, M. & Bouras, O., 2010. Removal of a neutral/anionic biocide from aqueous solutions using alginate encapsulated pillered clays. *Colloids and Surfaces A: Physicochemical and Engineering Aspects*. 366, 88-94.
- Mu, B. & Wang, A. 2016. Adsorption of dyes onto palygorskite and its composites: A review. *Journal of Environmental Chemical Engineering*, 4, 1274-1294.
- Namasivayam, C. & Arasi, D. J. S. E. 1997. Removal of congo red from wastewater by adsorption onto waste red mud. *Chemosphere*, 34, 401-417.
- Namasivayam, C. & Kanchana, N. 1992. Waste banana pith as adsorbent for color removal from wastewaters. *Chemosphere*, 25, 1691-1705.
- Namasivayam, C., Muniasamy, N., Gayatri, K., Rani, M. & Ranganathan, K. 1996. Removal of dyes from aqueous solutions by cellulosic waste orange peel. *Bioresource Technology*, 57, 37-43.
- Namasivayam, C. & Yamuna, R. T. 1992. Removal of congo red from aqueous solutions by biogas waste slurry. *Journal of Chemical Technology & Biotechnology*, 53, 153-157.
- Nandi, B. K., Goswami, A. & Purkait, M. K. 2008. Adsorption characteristics of brilliant green dye on kaolin. *Journal of Hazardous Matter*. 161, 387-395.
- Nandi, B. K., Goswami, A. & Purkait, M. K., 2009. Removal of cationic dyes from aqueous solutions by kaolin: Kinetic and equilibrium studies. *Applied clay science*, 42, 583 - 590.
- Ngulube, T., Gumbo, J. R., Masindi, V. & Maity, A. 2017. An update on synthetic dyes adsorption onto clay based minerals: A state-of-art review. *Journal of Environmental Management*, 191, 35-57.

- Nirmalarani, J. & Janardhanan, K., 1988. *Agricultural Journal*, 75, 41.
- Nwokonkwo 2013. Synthesis of 2-(1,3- Dihydro-3-Oxo- 2h - Pyridyrr -2- Ylidene) -1, 2 - Dihydro - 3h - Pyridylpyrrol - 3 - One. *IOSR Journal of Applied Chemistry*. 4(6), 74 - 78.
- Oladipo, A. A. & Gazi, M. 2014. Enhanced removal of crystal violet by low cost alginate/acid activated bentonite composite beads: optimization and modelling using non-linear regression technique. *Journal of Water Process Engineering*.2, 43-52.
- Ozcan, A., Oncii, E. & Ozcan, A., 2006. Adsorption of Acid Blue 193 from aqueous solution onto DEDMA-Sepiolite. *Journal of Hazard Matter*. 129, 244- 252.
- Pajootan, E., Arami, M. a. & Mohammad, N., 2012. Binary system dye removal by electrocoagulation from synthetic and real coloured wastewaters. *Journal of the Taiwan Institute of Chemical Engineers*, 43, 282-290.
- Panizza, M. & Cerisola, G. 2008. Removal of colour and COD from wastewater containing acid blue 22 by electrochemical oxidation. *Journal of Hazardous Materials*, 153, 83-88.
- Pereira & Alves 2012. Dyes - environmental impact and remediation. In: Malik A, Grohmann E (eds) *Environmental protection strategies for sustainable development, strategies for sustainability*. New York: Springer.
- Pollock, M. J., 1973. Neutralizing dyehouse wastes with flue gases and decolorizing with fly ash. *Amplified Dyestreatment Report*. 62, 21-23.
- Puranawari, N., Muthukrishnan, J. & Gunasekaran, P., 2006. *Indian Journal of experimental biology*, 44, 618-626.
- RAAG, 2000. Evaluation of risk based corrective action model. Canada, St John's, NL, Remediation Alternative Assessment Group, Memorial University of Newfoundland.
- Radha, K. V; Regupathi, I; Arunagiri, A; Murugesan, T, 2005. Decolorization studies of synthetic dyes using phanerochaete chrysosporium and their kinetics. *Journal of Biochem Process* 40, 3337-3345.

- Reddy, D. H. K. & Lee, S.-M. 2013. Application of magnetic chitosan composites for the removal of toxic metal and dyes from aqueous solutions. *Advances in Colloid and Interface Science*, 201–202, 68-93.
- Robinson, T., McMullan, G., Marchant, R. & Nigam, P., 2001. Remediation dyes from textile effluents: a critical review of current treatment technologies with a proposed alternative. *Bioresource Technology*. 77, 247-255.
- Roshan, S. 2015. Removal of Congo red dye from water using orange peel as an adsorbent. India: National Institute of Technology Rourkela-769008.
- Rui, G., Ye, J., Wei, D., Yan, X., Hu, J. & Xin, H. 2013. Adsorptive Removal of Methyl Orange and Methylene Blue from aqueous solution with Finger- Citron- Residue - Based Activated Carbon. *Indengchemres* 52, 14297- 14303.
- Sachdeva, S., Kumar, A., 2009. Preparation of nanoporous composite carbon membrane for separation of rhodamine B dye.. *Journal of Membrane Science*. 329, 2-10.
- Santos, S.C.R., Oliveira A.F.M., Boaventura. R.A.R., 2016. Bentonitic clay as adsorbent for the decolourisation of dyehouse effluents. *Journal of Cleaner Production*. 126, 667 – 676.
- Sarma, G.K., Gupta, S.S., Bhattacharyya, K.G., 2016. Adsorption of Crystal violet on raw and acid-treated montmorillonite, K10, in aqueous suspension. *Journal of Environmental Management*, 171, 1-10.
- Sasaki, K. & Moriyama, S. 2014. Effect of calcination temperature for magnesite on interaction of MgO-rich phases with boric acid. *Ceramics International*, 40, 1651-1660.
- Sasaki, K. & Moriyama, S. 2014. Effect of calcination temperature for magnesite on interaction of MgO-rich phases with boric acid. *Ceramics International*, 40, 1651-1660.
- Sasmal, D., Maity, J., Kolya, H. & Tripathy, T. 2017. Study of congo red dye removal from its aqueous solution using sulfated acrylamide and N, N- dimethyl acrylamide grafted amylopectin. *Journal of Water Process Engineering*, 18, 7-19.

- Schulze, D. i., J. B, D. & S. B, W. (., 1989. Minerals in Soil Environment, 2nd ed. Soil Science Society of America, Madison, 1.
- Sebastian, S., Mayadevi, S., Beevi, B. & Sujata Mandal, S., 2014. Layered Clay - Alginate Composites for the Adsorption of Anionic Dyes: A Biocompatible Solution for Water/ Wastewater Treatment. *Journal of Water Resource and Protection*, 6: 177-184.
- Shaban, M., Abukhadra, M. R., Khan, A. a. P. & Jibali, B. M. 2018. Removal of Congo red, methylene blue and Cr(VI) ions from water using natural serpentine. *Journal of the Taiwan Institute of Chemical Engineers*, 82, 102-116.
- Shaik, S., 2007. The lewis legacy; the chemical bond - a territory and heartland of chemistry. *Journal of Comput Chemistry* 28, 51 - 61.
- Shariatia, S., Farajib, M., Yamini, Y. & Rajabib, A., 2011. Fe<sub>3</sub>O<sub>4</sub> magnetic nanoparticles modified with sodium dodecyl sulfate for removal of safranin next term O dye from aqueous solution. *Desalination*, 270 : 160.
- Shenai, V. A., 1995. Azo dyes on textiles vs German ban, an objective assessment. *Chemistry Weekly* 12, 33-34.
- Singh & Bharati 2014. *Handbook of natural dyes and pigments*. New Delhi: Woodhead Publishing.
- Slokar, Y. & A. Majcen Le Marechal, 1998. Method of decolorization of textile wastewaters. *Dyes pigments*. 37, 335-356.
- Srinivasan, R. & Sorial, G. 2009. Treatment of perchlorate in drinking water: a critical review. *Separation Purification Technology*, 15, 201 - 208.
- Suteu, D., Coseri, S. & Rusu, L. 2016. Kinetics studies on the adsorption behaviour of Basic Blue 9 dye on macroporous ion exchanger resins. *Desalination and Water Treatment*, 57, 14665-14673.
- Tahir, M. A., Bhatti, H. N. & Iqbal, M., 2016. Solar red and Brittle Blue direct dyes adsorption onto *Eucalyptus angophoroides* bark: equilibrium, kinetics and thermodynamics studies. *Journal of Environmental and Chemical Engineering*. 4, 2431-2439.

- Tan, B. H., Teng, T. T. & Omar, A. K. M. 2000. Removal of dyes and industrial dye wastes by magnesium chloride. *Water Research*, 34, 597-601.
- Tan, K. B., Vakili, M., Horri, B. A., Poh, P. E., Abdullah, A. Z. & Salamatina, B. 2015. Adsorption of dyes by nanomaterials: Recent developments and adsorption mechanisms. *Separation and Purification Technology*, 150, 229-242.
- Toor, M. & Jin, B. 2012. Adsorption characteristics, isotherm, kinetics, and diffusion of modified natural bentonite for removing diazo dye. *Chemical Engineering Journal*, 187, 79-88.
- Toor, M., Jin, B., Dai, S. & Vimonses, V. 2015. Activating natural bentonite as a cost-effective adsorbent for removal of Congo-red in wastewater. *Journal of Industrial and Engineering Chemistry*, 21, 653-661.
- Tran, H. N., You, S.-J., Hosseini-Bandegharai, A. & Chao, H.-P. 2017. Mistakes and inconsistencies regarding adsorption of contaminants from aqueous solutions: A critical review. *Water Research*, 120, 88-116.
- V.A, S., 1995. Azo dyes on textile vs German ban, an objective assessment. *Chem. Weekly* 12, 33-34.
- Vakili, M., Rafatullah, M., Salamatina, B., Abdullah, A. Z., Ibrahim, M. H., Tan, K. B., Gholami, Z. & Amouzgar, P. 2014. Application of chitosan and its derivatives as adsorbents for dye removal from water and wastewater: A review. *Carbohydrate Polymers*, 113, 115-130.
- Venkataraman 1972. *The chemistry of synthetic dyes*, Vol. 7. New York: Academic press.
- Vhahangwele, M., Mugeru, W. G., Hlanganani, T. & Marinda, D. 2015. Efficiency of ball milled South African bentonite clay for remediation of acid mine drainage. *Water Process Engineering*, 8, 227 - 240.
- Vimonses, V., Lei, S., Jin, B., Chow, C. W. K. & Saint, C. 2009. Adsorption of congo red by three Australian kaolins. *Applied Clay Science*, 43, 465-472.

- Vu, M. T., Chao, H.-P., Van Trinh, T., Le, T. T., Lin, C.-C. & Tran, H. N. 2018. Removal of ammonium from groundwater using NaOH-treated activated carbon derived from corncob wastes: Batch and column experiments. *Journal of Cleaner Production*, 180, 560-570.
- Wang, L. & Wang, A. 2007. Adsorption characteristics of Congo Red onto the chitosan/montmorillonite nanocomposite. *Journal of Hazardous materials*, 147, 979-985.
- Wang, Q., Luan, Z., Wei, N., Li, J. & Liu, C. 2009. The color removal of dye wastewater by magnesium chloride/red mud (MRM) from aqueous solution. *Journal of Hazardous Materials*, 170, 690-698.
- Weng, C., Lin, Y. a. & Tzeng, T., 2009. Removal of methylene blue from aqueous solution by adsorption onto pineapple leaf powder. *Journal of Hazardous Materials*, 170, 417-424.
- Widjijanti 2009. Kajian penggunaan adsorben sebagai alternatif pengolahan limbah zat pewarna tekstil. *Proceeding seminar nasional kimia peningkatan kualitas pendidikan dan penelitian kimia menyongsong UNY sebagai world class university*. FMIPA Universitas Negeri Yogyakarta, 96 - 100.
- Xu, J., Xu, D., Zhu, B., Cheng, B. & Jiang, C. 2018. Adsorptive removal of an anionic dye Congo red by flower-like hierarchical magnesium oxide (MgO)-graphene oxide composite microspheres. *Applied Surface Science*, 435, 1136-1142.
- Xu, Y. & Lebrun, R. E, 1999. Treatment of textile dye plant effluent by nanofiltration membrane. *Separation Science Technology*. 34, 2501-2519.
- Yang, N., Zhu, S., Zhang, D. & Xu, S. 2008. Synthesis and properties of magnetic Fe<sub>3</sub>O<sub>4</sub>-activated carbon nanocomposite particles for dye removal. *Materials Letters*, 62, 645-647.
- Yola, M. L., Eren, T., Atar, N. & Wang, S. 2014. Adsorptive and photocatalytic removal of reactive dyes by silver nanoparticle-colemanite ore waste. *Chemical Engineering Journal*, 242, 333-340.

- Yue, Q.-. Y., Li, Q., Gao, B.-. Y. & Wang, Y., 2007. Kinetics of adsorption of disperse dyes by polyepichlorohydrin- dimethylamine cationic polymer/ bentonite. *Separation and Purification Technology*, 279- 290.
- Zehra, B; Yoldas, S; Levent, C, 2009. Removal of congo red by using an invasive marine alga *Caulerpa racemosa* var. *cylindracea*. *Journal of hazardous materials* 161, issues 2-3, 1454-1460.
- Zeynep, E. & Filiz, N., 2006. Adsorption of reactive Black 5 from an aqueous solution: equilibrium and kinetic studies. *Desalination* 194, 1- 10.
- Zhang, J., Yan, X., Hu, M., Hu, X. & Zhou, M. 2018. Adsorption of Congo red from aqueous solution using ZnO-modified SiO<sub>2</sub> nanospheres with rough surfaces. *Journal of Molecular Liquids*, 249, 772-778.
- Zhang, Q., 2010. Nanocolorants. In: Scatter KD (ed) *Handbook of nanophysics: Functional nanomaterials*. CRC Press, Tylor & Francis Group, New York.
- Zhao, S., Gao, B., Yue, Q. & Wang, Y. 2014. Effect of Enteromorpha polysaccharides on coagulation performance and kinetics for dye removal. *Colloids and Surfaces A: Physicochemical and Engineering Aspects*, 456, 253-260.
- Zhao, S. & Wang, Z. 2017. A loose nano-filtration membrane prepared by coating HPAN UF membrane with modified PEI for dye reuse and desalination. *Journal of Membrane Science*, 524, 214-224.
- Zheng, X., Li, X., Li, J., Wang, L., Jin, W., Liu, J., Pei, Y. & Tang, K. 2018. Efficient removal of anionic dye (Congo red) by dialdehyde microfibrillated cellulose/chitosan composite film with significantly improved stability in dye solution. *International Journal of Biological Macromolecules*, 107, 283-289.
- Ziane, S., Bessaha, F., Marouf-Khelifa, K. & Khelifa, A. 2018. Single and binary adsorption of reactive black 5 and Congo red on modified dolomite: Performance and mechanism. *Journal of Molecular Liquids*, 249, 1245-1253.
- Zollinger, H. *Color chemistry: Synthesis, properties, and applications of organic dyes and pigments*. 1991 New York, USA. VCH Publications.